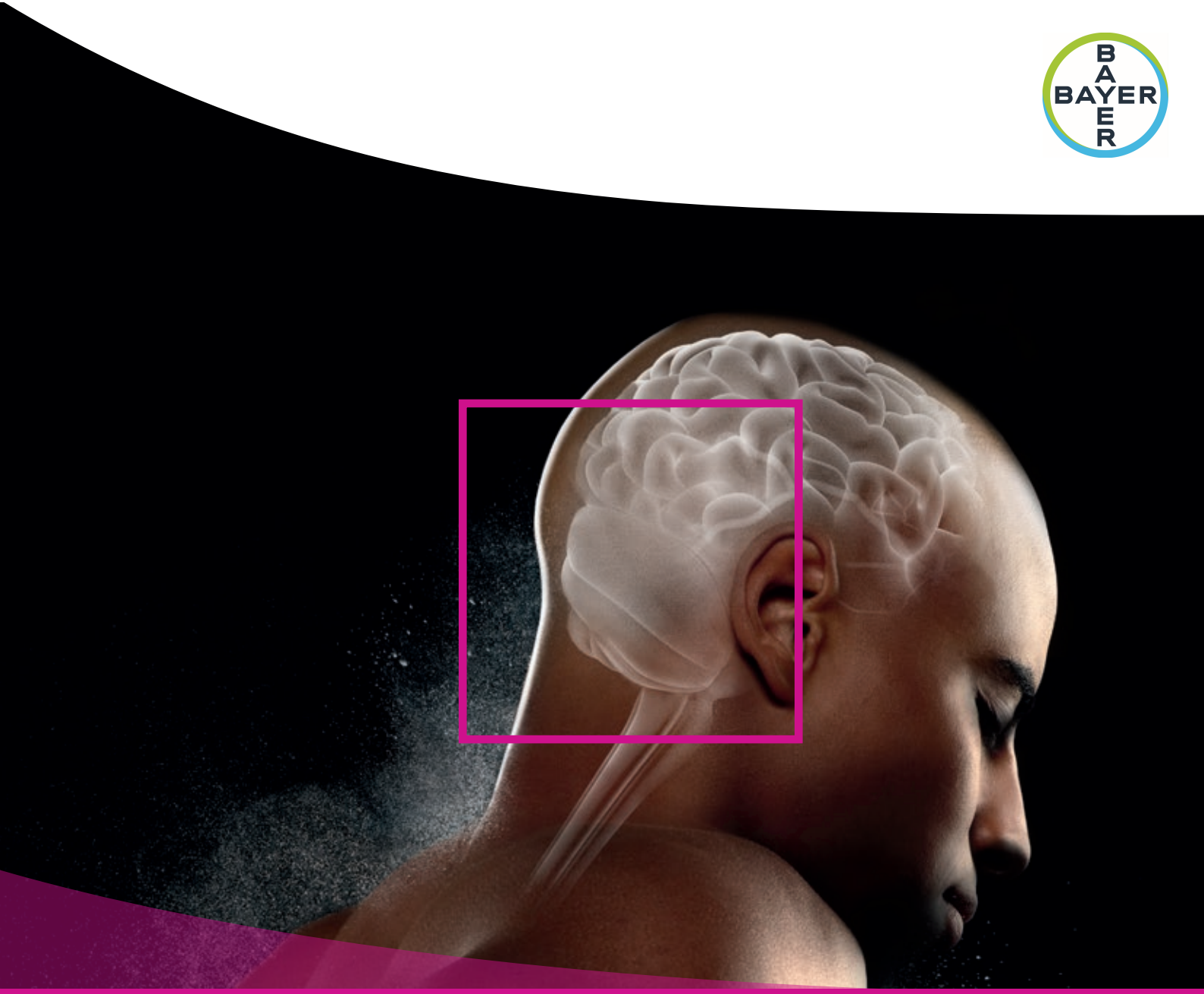

CNS: Tips and Tricks

Tips and Tricks for Gadovist® 1.0-Enhanced MRI and MRA of the CNS

Gadovist® 1.0
Gadobutrol

Table of Contents

Abbreviations

ADC apparent diffusion coefficient
ASL arterial spin labeling
AVM arteriovenous malformation
AVF arteriovenous fistula
b.w. body weight
CE contrast enhancement
CNR contrast-to-noise ratio
CT computed tomography
CTA computed tomographic angiography
DCE dynamic contrast-enhanced
DSA digital subtraction angiography
DSC dynamic susceptibility contrast
DTI diffusion tensor imaging
DWI diffusion-weighted imaging
EPI echo-planar imaging
ETL echo train length
FA flip angle
FFE fast field echo/field echo
FLAIR fluid-attenuated inversion recovery
FOV field of view
FSE fast spin echo
GBCA gadolinium-based contrast agent
Gd gadolinium
GRE gradient recalled echo
IV intravenous
MRA magnetic resonance angiography
MRI magnetic resonance imaging
MRS magnetic resonance spectroscopy
MS multiple sclerosis
MSD mean square difference
MT magnetization transfer
MTT mean transit time
NCE-MRA non-contrast enhanced magnetic resonance angiography
NEX number of excitations
PET positron-emission tomography
PWI perfusion-weighted imaging
rCBF relative cerebral blood flow
rCBV relative cerebral blood volume
SRS stereotactic radiosurgery
SWI susceptibility-weighted imaging
TE echo delay time
TI inversion time
TIA transient ischemic attack
TOF time of flight
TR relaxation time
TSE turbo spin echo
TTP time to peak
WBRT whole brain radiotherapy

Foreword

Aims of this Tips and Tricks brochure

CE-MRI is the gold-standard imaging modality for the diagnosis, classification, and treatment planning of multiple CNS pathologies. This brochure provides advice on the applications of CE-MRI in CNS imaging and practical information on the techniques that are involved.

Emphasis is given to the use of Gadovist® (gadobutrol) – a GBCA that is approved in adults and children of all ages including term neonates for CE-MRI of various body regions, including the brain and spine, head and neck region, lung, breast, abdomen, pelvis, kidney, extremities, and musculoskeletal system, as well as cardiac MRI to diagnose coronary heart disease, and contrast-enhanced MR angiography (MRA).* Gadovist® offers a unique combination of high (1 M) gadolinium concentration, high relaxivity, and high chelate stability that provide optimized imaging and safety characteristics proven in clinical trials, as described in this brochure (Frenzel et al. 2008; Huppertz and Rohrer 2004; Voth et al. 2011).

Organization of the Tips and Tricks brochure

The brochure is organized into sections that describe the applications and the techniques for use of Gadovist®-enhanced MRI and MRA in specific approved indications.

Each section consists of three units:

- An overview of CE-MRI and the specific applications of Gadovist®-enhanced MRI
- Practical tips and tricks to optimize Gadovist® use, and
- Case studies to demonstrate Gadovist® use in practice

Supportive references are provided throughout the brochure.

Acknowledgments

This Tips and Tricks brochure has been developed under the guidance of Marco Essig (University of Manitoba, Winnipeg) and Àlex Rovira (Vall d'Hebron University Hospital, Barcelona), who are expert clinical neuroradiologists with extensive practical experience. The contribution of cases from various clinical centers is highly acknowledged.

* Note to readers: Please check the most up-to-date information for the approved indications of Gadovist® in your location.

Introduction to CE-MRI and CE-MRA of the CNS

Standard CE-MRI

MRI is the most widely used modality for imaging CNS lesions and malformations. Contrast enhancement by the addition of a GBCA to MRI protocols can improve image quality, providing superior detection and characterization of lesions and malformations – relevant to diagnosis, classification, and therapeutic monitoring.

Sequences in a standard CE-MRI protocol should include:

- T1 weighted pre-contrast imaging
- T2 weighted spin-echo (pre- or post-contrast or both)
- T2-FLAIR (pre- or post-contrast, depending on protocol preference)
- T1-weighted contrast imaging

Advanced MRI techniques

Advanced MRI techniques can complement standard CE-MRI by visualizing functional tissue characteristics and vascularization status, providing additional information on differential diagnosis, lesion grade, and (for tumors) malignant potential (Essig et al. 2013b; Law et al. 2002).

Advances in acquisition techniques, data processing, and equipment are increasing the applications of advanced MRI to areas where other modalities were preferred in the past, e.g., stroke.

Commonly used advanced imaging techniques that use GBCA include DSC and DCE, which can be combined in the same protocol.

Image acquisition techniques and post-processing algorithms remain very individual in different institutions.

DSC MRI (perfusion imaging)

DSC MR perfusion, also known as “bolus tracking MRI” or “perfusion-weighted imaging”, is a technique in which the first pass of a bolus of GBCA through brain tissue is monitored by a reduction in signal intensity on a series of GRE or Echo-planar imaging (EPI) T2*-weighted MR images. Acquired data are post-processed to obtain perfusion maps with parameters including rCBV rCBF, MTT, and TTP. Examples of acquisition parameters in DSC MRI are shown in Table 1.1.

Parameter	Range of value
Acquisition time	45 to 60 sec, can go up to 3 min
Number of repeated images at each slice	32–80, high number is better for good baseline characterization
TR	1–2 s, need good temporal resolution for sufficient sampling
TE	50-80, about the same as the T2
FOV	20 × 20 to 24 × 24 cm
Matric	128 × 128 is a good compromise on temporal and spatial resolution
Slice thickness	2 to 10 mm depending on the need for whole brain coverage
In-plane spatial resolution	2 mm

Table 1.1 DSC image acquisition parameters

Parameter	Range of value
Acquisition time	Depends on the parameters to be measured › 3 min for Ktrans › Up to 6-7 minutes for Vp, Ve, and Kep assessments
Matrix	128 × 128
Slice thickness	2–10 mm depending on spatial coverage
Spatial resolution	1 mm in-plane × 5 mm slices
Temporal resolution of the single T1 acquisition	3.5 to 6 sec, depending on the specific scanner hardware and field strength

Table 1.2 DCE image acquisition parameters (spoiled GRE) (Essig et al. 2013b; Paldino and Barboriak 2009)

DCE MRI (permeability imaging)

DCE MR perfusion, also widely referred to as “permeability” or “pharmacokinetic” MRI, is based on the acquisition of serial T1-weighted images before, during, and after administration of extracellular low-molecular-weight MR contrast media, such as a GBCA. The resulting signal intensity–time curve reflects a composite of tissue perfusion, tissue vascularity, vessel permeability, and extravascular-extracellular space (Essig et al. 2013b)

Acquired data is post-processed to obtain permeability maps such as Ktrans, which reflects a combination of tumor blood flow and microvascular permeability; Ve, which measures the extravascular extracellular space volume fraction; Vp, which measures the plasma volume fraction; and Kep (K_{trans} /Ve), which is a rate constant that measures the transfer of contrast agent from the extravascular extracellular space to plasma.

- Examples of acquisition parameters for DCE MRI are shown in Table 1.2
- Sequence: typically 3D SPGR/MPRAGE/FLASH/FFE

CE-MRA

MRA uses a magnetic field and pulses of radio wave energy to provide accurate visualization of the intracranial and extracranial vasculature and angioarchitecture. MRA offers the advantages of speed of acquisition, high image quality, and robust results.

Acquisition techniques include:

- Flow-dependent MRA, e.g., TOF, phase-contrast
- Flow-independent MRA, e.g., CE-MRA

3D TOF and 3D CE-MRA are standard methods for the assessment of cerebral vessel patency and angioarchitecture

- Applications include cerebrovascular manifestations of atherosclerotic disease or thrombus, intracranial aneurysms, venous drainage of tumors (Wikström et al. 2008)

4D MRA techniques provide 3D visualization of the vessel network and tracking of contrast bolus through the vessels over time (Hadizadeh et al. 2012).

High-resolution techniques of vessel imaging at 7.0-T MRI using 3D TSE sequence has also recently been developed (using Gadovist® as the contrast agent)(Clevert et al. 2006).

Standard sequences for intracranial MRA protocol are:

- Precontrast 3D-TOF. Commonly used for intracranial arterial MRA
- Contrast-enhanced MRA – T1-weighted 3D spoiled GRE or 3D fast imaging with steady precession (FISP). Commonly used for supra-aortic vessels
- Contrast-enhanced 3D-TOF

Technique	Low cost	Minimal time required	No/few flow artifacts	Non-invasive	No exposure to ionizing radiation
DSA	×	×	√	××	×
CTA	√	√√	×	√	×
NCE-MRA	√	××	×	√	√
CE-MRA	√	√	√	√	√

Table 1.3 Relative advantages and disadvantages of vasculature imaging techniques

MRA versus DSA and CT angiography (Table 1.3)

Key benefits of MRA versus DSA and CT angiography are:

- Non-invasive: no need for arterial puncture or manipulation, as with DSA (Lawson et al. 2011)
- No exposure of patients to ionizing radiation or iodinated contrast agents, as with DSA and CTA (Forsting and Palkowitsch 2010; Olin et al. 2004)
- Advanced dynamic imaging techniques available; not possible with CTA

Power injector use

Use of a power injector is recommended – particularly for advanced imaging techniques that require precise GBCA administration (Essig et al. 2013b).

Gadovist® is administered by power injector at a rate of approximately 2.0 mL/sec, up to 5.0 mL/sec (perfusion imaging), followed immediately by a saline flush of 25 mL (range, 10–30 mL), injected at the same rate as the Gadovist® bolus (Anzalone 2010; Essig et al. 2013b). For MRA, the rate of Gadovist® injection may be slower.

Consistent delivery of Gadovist® by a power injector has the following advantages (Essig et al. 2013b):

- Standardized and reproducible volume
- Precise timing
- Tight bolus
- Consistency in adherence to protocols
- Ease of use

Primary and Metastatic Tumors of the Brain and Spine

Role of CE-MRI

Standard MRI

CE-MRI is the imaging modality of choice for the identification, differential diagnosis, grading, and treatment planning of primary CNS lesions, including gliomas and meningiomas, and metastases, with superior sensitivity compared with alternative imaging modalities (Essig et al. 2012).

CE-MRI is superior to CT for detection of small lesions, with the advantages of good soft tissue contrast, absence of bone artifacts, few partial volume effects, and direct multiplanar imaging (Bauknecht et al. 2010; Fries et al. 2009; Seute et al. 2008; Tsao et al. 2012).

Advanced imaging

Advanced MRI techniques complement standard CE-MRI by visualizing functional tissue characteristics and the vascularization status in tumor tissue, providing additional information for differential diagnosis, grade, and malignant potential (Essig et al. 2012).

Perfusion studies that calculate rCBF and rCBV can be used to monitor response to therapy and predict progression (Essig et al. 2004; Law et al. 2006).

Applications of Gadovist®-enhanced MRI

Standard MRI

- Lesion localization, identification, delineation, and characterization
- Guidance on therapy

Advanced imaging

- Lesion localization, identification, delineation, and characterization
- Post-therapeutic response assessment

Tips and Tricks to optimize Gadovist®-enhanced MRI of primary and metastatic tumors

Tip one: General protocol recommendations

Gadovist® dose

- The standard Gadovist® dose to characterize CNS lesions is 0.1 mmol/kg b.w., which can be used in most circumstances (Breuer et al. 2013)
- Additional Gadovist® doses up to 0.2 or 0.3 mmol/kg b.w. are advantageous in cases of diagnostic doubt, by increasing tumor visualization/conspicuity and lesion detection rates, e.g., to identify small foci or to exclude additional lesions (Anzalone et al. 2009; Anzalone et al. 2013b; Engelhorn and Doerfler 2008; Essig et al. 2012; Kim et al. 2010)
- The standard Gadovist® dose should not be exceeded in patients with glomerular filtration rate <30 mL/min/1.73 m^2 (Anzalone 2010)

Field strength

- Minimum 1.5 T
- Higher field strengths (e.g., 3 T) provide superior image quality, if available (Essig et al. 2012)

Image acquisition

- Delay can be built in to the protocol by performing DWI and/or DTI before T1 contrast enhanced sequences
- T2-FLAIR sequences can be acquired post-contrast
- Delayed postcontrast imaging is recommended (particularly for metastases), to improve lesion detection rates and assessment of lesion volume (Essig et al. 2012)
- Magnetization transfer sequences – to better visualize metastatic lesions (Elster et al. 1994; Finelli et al. 1994; Gillams et al. 1996)

Tip two: Gadovist®-enhanced MRI of primary brain lesions: protocol elements

Standard imaging

Recommended standard protocol elements for Gadovist®-enhanced MRI of primary brain tumors are shown in Table 2.1.

Advanced imaging

Advanced imaging techniques are increasingly incorporated into routine protocols for Gadovist®-enhanced MRI.

Standardization of acquired perfusion parameters is essential for consistency in tumor grading and assessment of prognosis and treatment response (Essig et al. 2013a; Shiroishi and Lacerda 2010).

With use of modern techniques, e.g., high-relaxivity and high-concentration contrast media such as Gadovist®, in combination with high-end MRI equipment, a single dose of contrast medium can be split into two injections (Essig et al. 2012).

Recommended advanced protocol elements for Gadovist®-enhanced MRI of primary brain tumors are shown in Table 2.1.

Integrated protocols

An integrated sequence for combining standard and advanced protocols for Gadovist®-enhanced MRI is shown in Figure 2.1.

Optimization of protocol sequence enhances lesion visualization and characterization.

Standard	Advanced
3-Plane localizer/scout	T1 map (quantitation) for DCE MR imaging—3D gradient-echo T1 or 2D TSE/FSE T1
T1-weighted precontrast (SE)	DWI and/or DTI (can extract DWI data trace/ADC from DTI)
T2-weighted axial (optional post-injection)	T2* DSC MR imaging (after presaturation DCE MR imaging sequence)
T2-FLAIR (postcontrast injection provides better sensitivity for meningeal/ependymal spread)	Functional language, auditory, visual, motor testing, and MRS^
3D volumetric T1-weighted postcontrast (GRE) – for radiosurgical or neuro-navigation planning	SWI, gradient-echo, additional optional sequences
T1-weighted postcontrast (SE)	

Table 2.1 Elements of imaging protocols for Gadovist®-enhanced MRI of primary brain tumors (Essig et al. 2012)

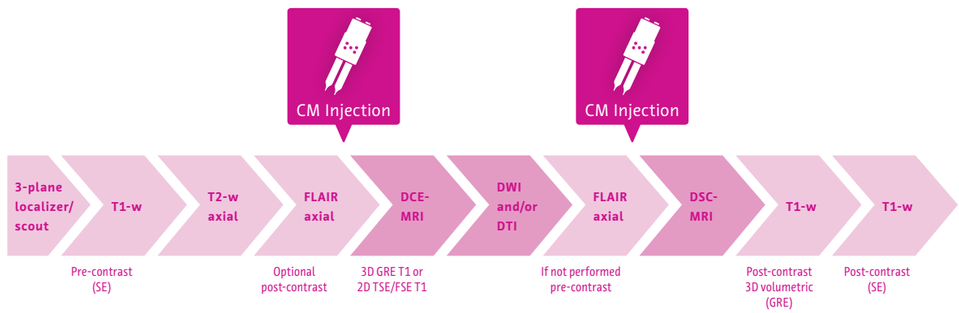

Figure 2.1 Integrated standard and advanced protocol for Gadovist®-enhanced MRI of primary brain tumors (Essig et al. 2012)

Standard	Advanced
Pretreatment MR assessment	
› T1-weighted pre-contrast imaging	› Magnetization transfer contrast – optional
› T2-weighted spin-echo	
› Post-contrast T2-FLAIR - to detect meningeal spread of disease	
Follow-up MR assessment post-SRS	
› T1-weighted postcontrast (SE)	› Dynamic contrast-enhanced MRI–optional
› T2-weighted spin-echo	› Dynamic susceptibility-weighted contrast-enhanced MRI–optional
› 3D GE T1-weighted contrast imaging	› MRS and magnetization transfer contrast–optional
› Post-contrast T2-FLAIR	

Table 2.2 Elements of imaging protocols for Gadovist®-enhanced MRI of brain metastases (Anzalone et al. 2013a)

Tip three: Gadovist®-enhanced MRI of CNS metastases: protocol elements

Standard and advanced imaging

Recommendations of standard and advanced imaging protocol elements for Gadovist®-enhanced MRI of metastatic brain tumors are shown in Table 2.2.

Integrated protocols

An integrated sequence for combining standard and advanced protocols for Gadovist®-enhanced MRI of brain metastases is shown in Figure 2.2.

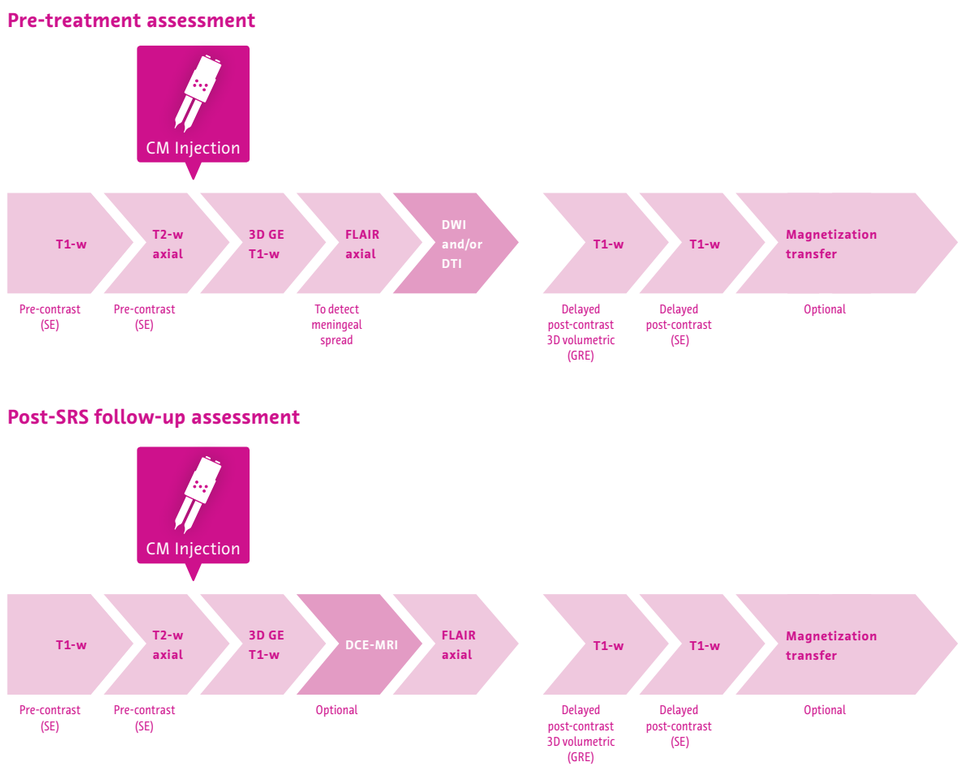

Figure 2.2 Integrated standard and advanced protocol for Gadovist®-enhanced MRI of metastatic brain tumors (Anzalone et al. 2013a)

Case 1: Glioblastoma

Primary and metastatic tumors of the brain and spine

Patient History

70-year-old female presenting with seizure and known breast cancer. She had a prior event of aphasia. An initial brain-CT showed partially hemorrhagic lesion, categorized as metastasis.

MRI Findings

MR images showed increased regional blood-volume (rCBV) close to CM-enhancing tumor.

Final Diagnosis

Partially hemorrhagic glioblastoma.

Patient Outcome

A glioblastoma was histopathologically confirmed by stereotactical biopsy. Due to the tumor's location in the speech area, the patient underwent radiation therapy instead of surgery.

Take-Home Message

MR perfusion helps to detect the underlying pathology in acute atypical brain bleeding or necrotic lesions. Increased rCBV indicates tumor angiogenesis typical for malignant glioma. Diffuse expansion of hyper-vascularization helps to differentiate between infiltrating gliomas and metastases (metastases always grow focal).

MR unit		
MR scanner	Siemens Healthcare, Verio	
Operating field strength (T)	3.0	
Coil	TIM Head Coil	
Injection protocol		
Injection system	MEDRAD® Spectris Solaris EP	
	Volume (mL)	**Flow rate (mL/s)**
Gadovist® 1.0	7.5	5
Saline	15	5
Bolus timing technique	Simultaneous start of injection & measurement	
Sequences	**Gadovist® 1.0**	**Gadovist® 1.0**
Sequence	EPI-2D T2*-Perfusion	T1 SE post KM
Start of scan p.i.	Sim	2-3min
Parallel imaging	Grappa 2	–
Fat saturation	Yes	No
Respiratory state	Free	Free
TR (ms)	1,500	455
TE (ms)	30	12
FA (deg)	90	70 & 180
FOV (mm)	230	240
RFOV or Phase FOV (%)	100	75
Matrix	EPI-2D T2*-Perfusion	T1 SE post KM
Slice orientation	Transversal	Transversal
Slice thickness (mm)	4	5
Slice gap (mm)	30%	30%
No. of slices	19	20
No. of measurements	50	2
Bandwidth (Hz/pixel)	1,446	80
k-space ordering	Lin	Lin
Subtraction	No	No
Acquisition time (min)	50 × 1.5s = 1:23	3:34

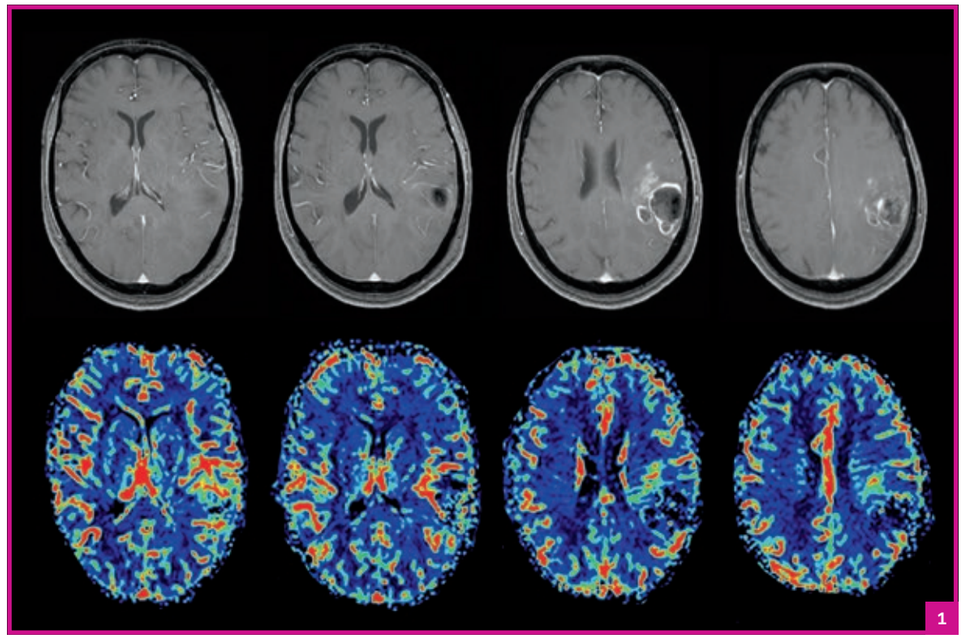

1 Increased regional blood-volume (rCBV) close to the bordering CM-enhancing tumor highly suspicious of malignant glioblastoma.

Courtesy of Elke Hattingen,
Johann-Wolfgang-Goethe-University, Frankfurt/Main, Germany

Case 2: Glioma

Primary and metastatic tumors of the brain and spine

Patient History

38-year-old female, 80 kg, presenting with seizures. She does not have any pre-exisiting medical conditions. She is now admitted for evaluation of a lesion-possible cavernous malformation.

MRI Findings

MR imaging shows an infiltrating mass lesion, initially thought to be cavernoma. Routine, contrast enhanced and DSC/DCE imaging are more consistent with moderate grade glioma.

Final Diagnosis

Grade II-III glioma.

Patient Outcome

Pathology proven by biopsy.

MR unit		
MR scanner (manufacturer & type)	GE 3t 750	
Operating field strength (T)	3.0	
Coils	8 channel head	
Injection protocol		
	Volume (mL)	**Flow rate (mL/s)**
Gadovist® 1.0	8	4
Saline	10	2
Sequences	**Gadovist® 1.0**	**Gadovist® 1.0**
Sequence	DSC	DCE
TR (ms)	1,500	820
TE (ms)	13	8
FA (deg)	60	90
FOV	22	22
Matrix	96×128	256×160
Slice thickness (mm)	5	5
Acquisition time (min)	60 s	4:31

Take-Home Message

Advanced physiologic imaging with perfusion and permeability can assist with lesion characterization. DSC and DCE imaging suggest the diagnosis of glioma, changing management to biopsy and treatment.

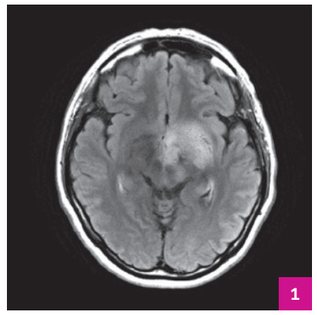

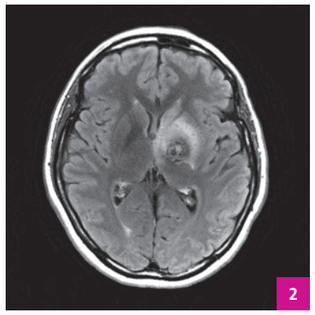

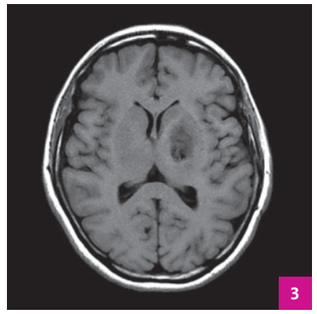

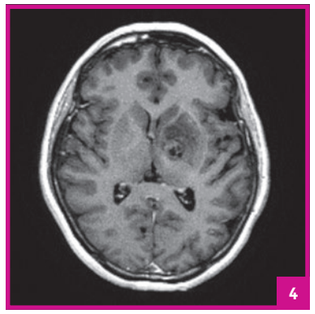

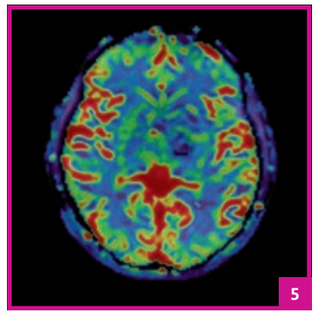

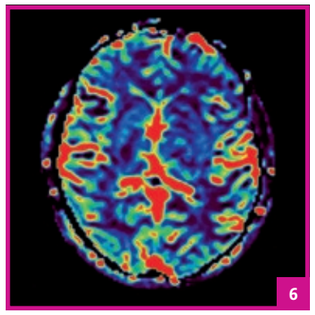

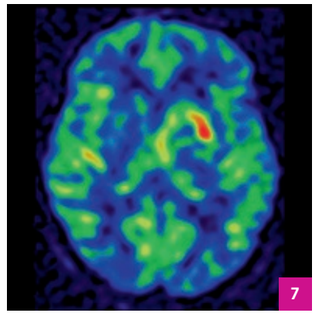

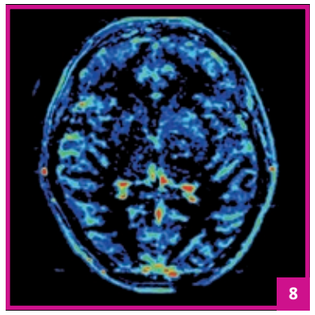

1 Flair propeller. Lesion extending from the uncus inferiorly through the corona radiata. Evidence of hemorrhage suggesting cavernoma. Overall appearance consistent with glioma.
2 T2 propeller. Left basal ganglia lesion suggesting hemorrhage. Potentially representative of cavernoma, but more consistent with glioma.
3 T1 FLAIR pre contrast. Left basal ganglia lesion mass.
4 T1 flair post contrast . No significant enhancement. Potentially cavernoma, but more consistent with glioma.
5–6 DSC CBF CBV. Subtle elevation of CBF CBV. Consistent with tumor.
7 ASL, ASL_FLAIR. High CBF within tissue adjacent to hemorrhage. High CBF values consistent with tumor.
8 T1 FSE DCE. Small focus of rapid vascular phase enhancement / high Ktrans. Suggestive of tumor neovascularity.

Courtesy of Lawrence N. Tanenbaum, Mount Sinai Hospital, New York/NY, USA

Case 3: Supratentorial Brain Tumor

Primary and metastatic tumors of the brain and spine

Patient History

3-year-old male with mild head trauma 5 weeks ago. The patient shows recurrent ataxia, vomiting and somnolence since 2 weeks.

MRI Findings

MRI images show inhomogeneous Gadovist® 1.0 enhancement in the tumor with cysts and blurring to the surrounding parenchyma.

Final Diagnosis

Supratentorial PNET (Primitive NeuroEctodermal Tumor).

Take-Home Message

Supratentorial PNETs are rare hemispheric brain tumors. PNETs commonly occur fronto-parietal with their center in the deep white matter. Gadovist® 1.0 has very good safety and tolerability in children. Only low contrast volume and injection pressure are needed.

MR unit		
MR scanner	SIEMENS, MAGNETOM Avanto	
Operating field strength (T)	1.5	
Injection protocol		
Injection system	Manual	
	Volume (mL)	**Flow rate (mL /s)**
Gadovist® 1.0	1	1
Saline	10	1

Sequences	Native	Native	Gadovist® 1.0	Gadovist® 1.0	Gadovist® 1.0
Sequence	T2-TSE	T1-SE	T1-SE	T1-SE	T1-SE
Respiratory state	Free breathing	Free breathing	Free breathing	Free breathing	Free breathing
TR (ms)	3,700	570	570	520	600
TE (ms)	81	13	13	8	11
TI (ms)	0	0	0	0	0
FA (deg)	150	90	90	90	90
FOV (mm)	190	157	157	135	189
RFOV or Phase FOV (%)	70.31	70	70	70.31	85.94
Matrix	270×384	224×320	224×320	360×512	330×384

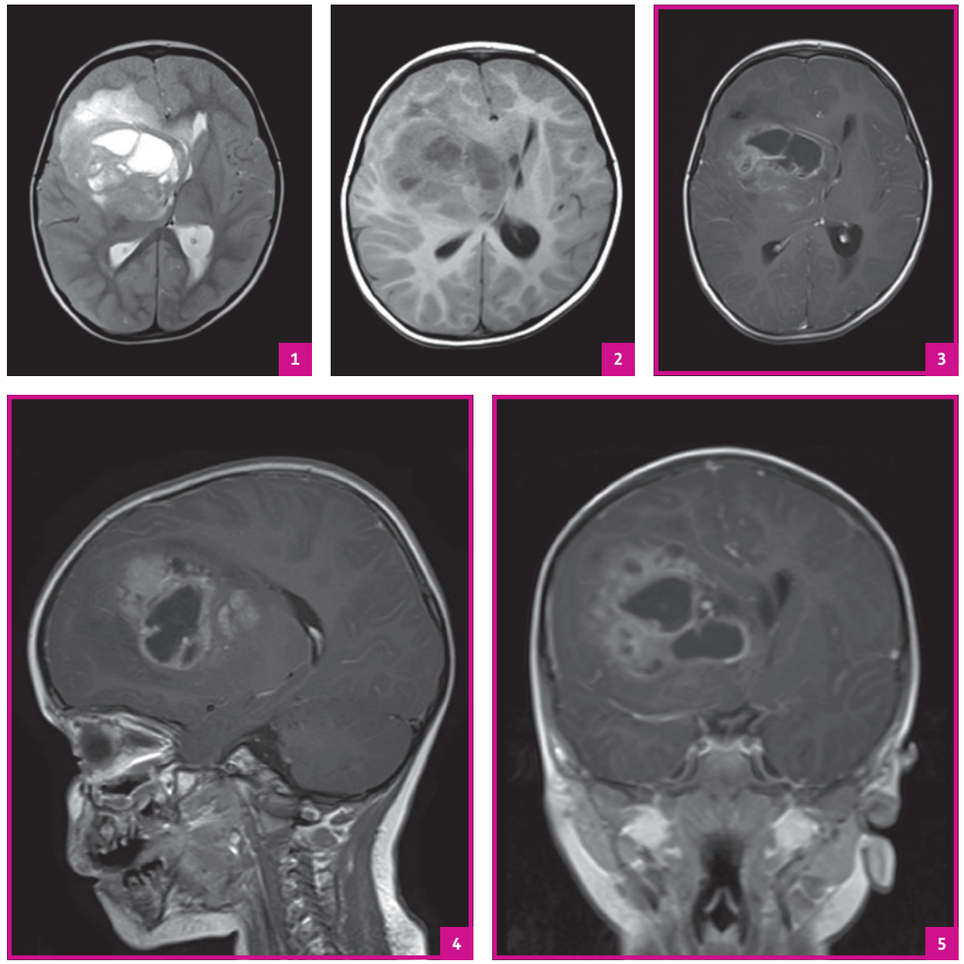

1–3 Compression of the I. and II. ventricel and displacement of the midline to left.
1 Pre-contrast T2-weighted images showed a large supratentorial brain tumor with inhomogeneous signal in the right hemisphere. Surrounding parenchyma of the right hemisphere shows bright signal in T2.
2 Pre-contrast T1-weighed images shows a large hypointense and cystic mass in the right frontal lobe.
3–5 Post-contrast: inhomogenous moderate enhancement in the solid portion of the tumor with cysts and blurring to the surrounding parenchyma.

Courtesy of Gabriele Hahn,
Carl Gustav Carus University Hospital, Dresden, Germany

Case 4: Optic Nerve Glioma

Primary and metastatic tumors of the brain and spine

Patient History

4-year-old girl with a skull diameter beyond 97th percentile presents with more than 6 café-au-lait spots. Neurofibromatosis is suspected.

MRI Findings

MR images show thickening of both optic nerves left > right, plump chiasm, multiple T2 hyperintense lesions, widening of perioptic cerebrospinal fluid spaces, enhancement of optic nerve gliomas left > right, and slight optic chiasm enhancement.

Final Diagnosis

The final diagnosis was bilateral optic nerve glioma extending into the optic chiasm in patient with neurofibromatosis.

Take-Home Message

Contrast-enhanced coronal sections of the orbit with fat suppression are particularly helpful in discerning optic nerve enhancement.

MR unit		
MR scanner	Siemens Avanto, SQ engine	
Operating field strength (T)	1.5	
Coil	32 Channel Head Coil	
Injection protocol		
Injection system	Manual	
	Volume (mL)	**Flow rate (mL /s)**
Gadovist® 1.0	2.8	~ 0.5
Saline	–	–

Sequences	Native	Native	Gadovist® 1.0	Gadovist® 1.0
Sequence	T2	T2	T1	3D FLASH (reformatted)
Fat saturation	No	Yes	Yes	Reformatted
Respiratory state	Free	Free	Free	image
TR (ms)	4,964	5,800	504	from
TE (ms)	98	101	11	sagittal
TI (ms)	–	–	–	3D series
FA (deg)	150	150	150	–
FOV (mm)	191×220	180	180	256
RFOV or Phase FOV (%)	87	100	100	–

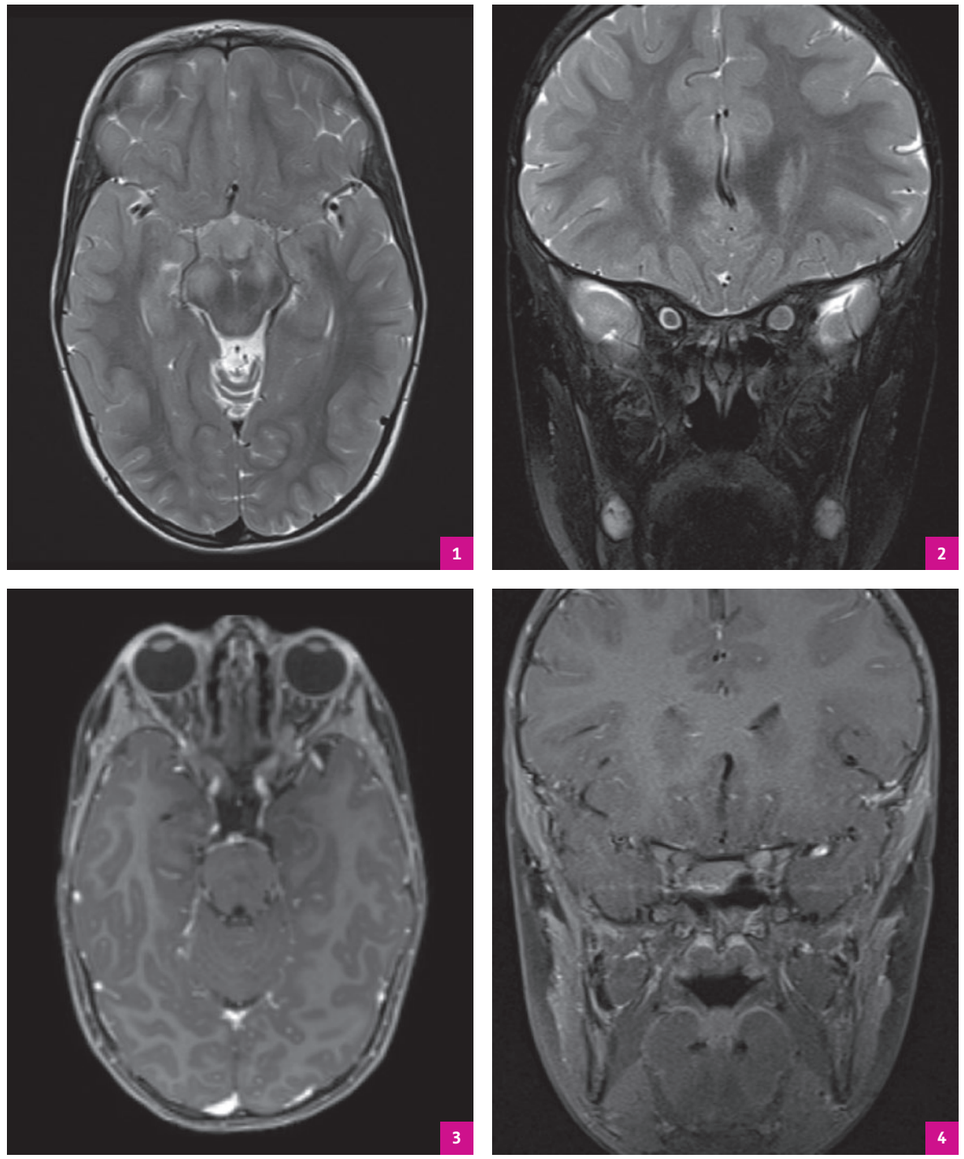

3–4 Multiple T2 hyperintense lesions. Enhancement of optic nerve gliomas, left > right. Slight enhancement of optic chiasm.

Courtesy of Christoph Ozdoba, MD,
Inselspital, University of Bern, Switzerland

Case 5: Metastatic Melanoma

Primary and metastatic tumors of the brain and spine

Patient History

69-year-old female, 57 kg, presenting with confusion, expressive aphasia, dysarthria, left upper motor neuron facial weakness, left arm and leg weakness. She does not have any other preexisting medical conditions. She has a skin lesion in the right temple.

MRI Findings

An initially suspected hemorrhagic lesion was detected as neoplasm. Structural and dynamic contrast enhanced MRI revealed an underlying enhancing mass in the right frontal lobe, suspicious for metastasis or glioblastoma multiforme (GBM).

Final Diagnosis

Metastatic melanoma in the right frontal lobe.

Patient Outcome

MRI prompted the patient to undergo a full metastatic workup and surgical resection.

Take-Home Message

In patients with a new hemorrhagic lesion, contrast-enhanced MRI is necessary to determine if there is an underlying neoplasm. Dynamic Gadovist® 1.0-enhanced MR perfusion is more useful than DSC-MR perfusion in the presence of hemorrhage as it is not limited by susceptibility artifacts.

MR unit		
MR scanner	Siemens Trio	
Operating field strength (T)	3.0	
Coil	32 Channel Head Coil	
Injection protocol		
Injection system	Power Injector	
	Volume (mL)	**Flow rate (mL/s)**
Gadovist® 1.0	5	2
Saline	20	2
Gadovist® 1.0	5	5
Saline	20	5
Sequences	**DSC**	**DCE**
Sequence	EPI-2D GRE	FLASH3D
TR (ms)	2,380	6.5
TE (ms)	54	TE1 1.65 TE2 3.85
FA (deg)	90	30
FOV (mm)	220	220
Matrix	128×86	128×86
Slice thickness	5	5
Acquisition time (min)	2:05	4:42

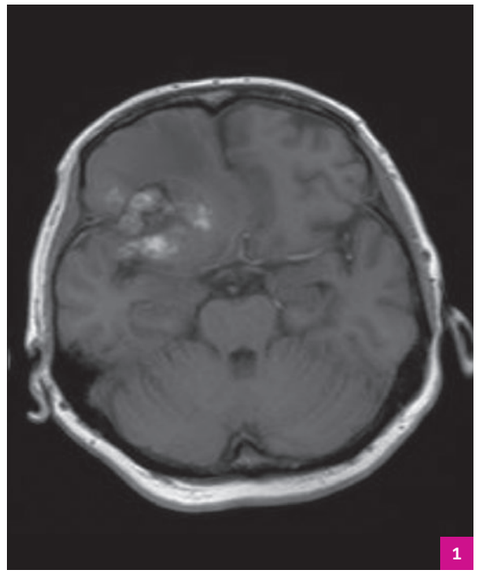

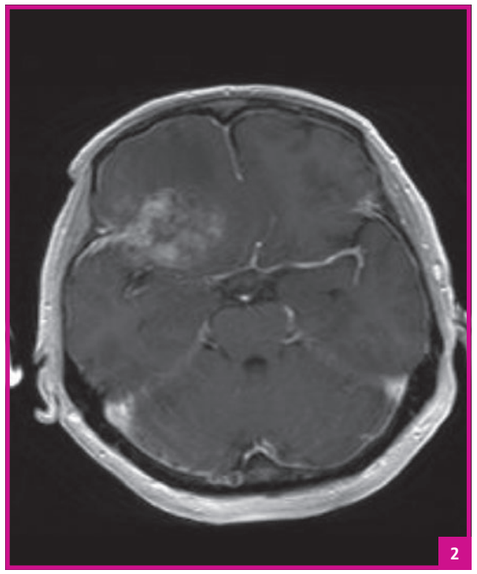

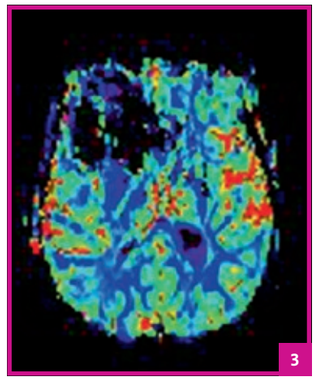

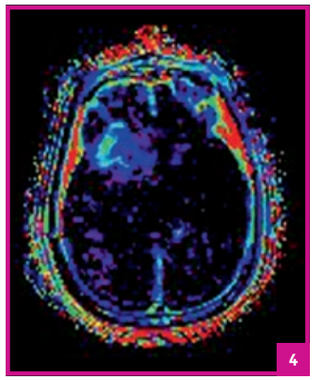

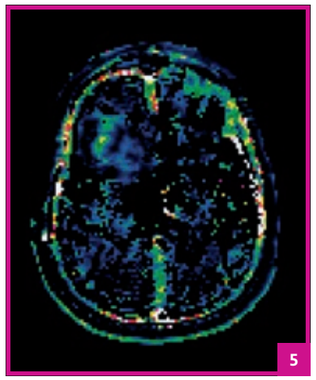

1 T1 FLASH pre contrast. Hemorrhagic lesion in the right frontal lobe causing subfalcine herniation to the left.
2 T1 FLASH post contrast. Patchy enhancement in the periphery of the hematoma.
3 rCBV computed from DSC GRE-T2* EPI perfusion. Hemorrhage within the mass causing susceptibility artifacts on gradient-echo perfusion images. Relative CBV measurement within the tumor is not possible with DSC GRE-T2*EPI.
4 Ktrans computed from DCE-MRI perfusion using 3D FLASH sequence. Areas of high Ktrans value at the lateral lesion edge. Increase in Ktrans due to an underlying tumor causing a leakage of the blood-brain barrier.
5 CBV computed from DCE-MRI perfusion with 3D FLASH sequence. Areas of high CBV value at the lateral lesion edge. Increase in CBV due to an underlying tumor, which could not be measured with DSC-MR perfusion imaging.

Courtesy of Thanh Binh Nguyen,
The Ottawa Hospital, Ottawa, Canada

Vascular Disease: Stroke and Vascular Malformations

Role of CE-MRI

Stroke

MR imaging: Identification and grading of ischemic events and progression over time

MRI has high sensitivity (superior to CT) for the detection of early infarction with ability to define the infarct core (Essig et al. 2013a; Fiebach et al. 2002; Kidwell et al. 2004; Saur et al. 2003; Schellinger et al. 2010).

- T2*-weighted GRE or SWI is performed for detecting intracranial hemorrhage
- DWI is a sensitive method for detecting hyperacute ischemia (Fiebach et al. 2002; Saur et al. 2003)
- DSC can estimate the location and extent of hypoperfused brain parenchyma (Essig et al. 2013a)
- DSC and DCE can distinguish reversibly and irreversibly injured tissue
- DWI and PWI in combination can define the location and extent of ischemia and infarction within minutes of onset (Wintermark et al. 2008). In series, the techniques can describe the evolution of ischemic lesions, identify ischemically threatened cerebral tissue amenable to therapeutic intervention, and monitor the effects of treatment (diffusion-perfusion mismatch) (Duong and Fisher 2004; Lansberg et al. 2007; Lansberg et al. 2011; Nagakane et al. 2011)

MR imaging: Response to treatment

Accurate evaluation of the ischemic penumbra by MRI has potential to target reperfusion therapy with greater precision (Essig et al. 2013a). MRI-guided thrombolysis is safer and potentially more effective than standard CT-based thrombolysis (Schellinger et al. 2010).

MRA

- 3D TOF is used for assessment of intracranial arteries
- CE-MRA is an established imaging technique to evaluate the atherosclerotic pathology of carotid and vertebrobasilar arteries (Menke 2009) and is a valuable supplement to digital subtraction angiography, with the ability to provide a comprehensive, non-invasive evaluation of the head and neck arteries in a single study (Yang et al. 2005)
- CE-MRA is increasingly included in standard protocols for the diagnosis of acute stroke, with ability to locate sources of thrombi or emboli and identify sites for thrombolytic treatment (Essig and Tanenbaum 2013)
  - CE-MRA visualizes distal vessels with faster image acquisition than TOF MRA (Alfke et al. 2011)
- CE-MRA can be used alongside PWI to diagnose intravascular occlusion due to thrombus or atherosclerotic plaque and to evaluate carotid bifurcation and vertebrobasilar system in patients with acute stroke (Byrnes and Ross 2012)

Vascular malformations

MRA

CE-MRA provides detailed images of the location, feeding vessels, and drainage patterns of vascular malformations – including capillary telangiectasias, developmental venous anomalies, cavernous malformations, AVMs, and AVF (Essig and Tanenbaum 2013).

Applications of Gadovist®-enhanced MRI

Stroke

Advanced imaging

- Detect early ischemia
- Define the location and extent of ischemia – define the presence of perfusion- diffusion mismatch
- Target the location of perfusion therapy

MRA

- Presence and degree of atherosclerotic disease or other underlying vascular pathology (e.g., dissection) or aneurysmatic changes
- Location of thrombi

Vascular malformations

Standard CE-MRI

- Detect vascular malformations and describe their angioarchitecture
- Detect secondary changes of vascular malformations
- Differentiate from highly vascularized tumors

Advanced imaging

- Differential diagnosis – e.g., vascular lesions – tumors
- Quantify changes of the adjacent normal tissue
- Define the hemodynamic changes of the cerebral vasculature due to the malformation

MRA

- Location, feeding vessels, and drainage patterns of vascular malformations
- Treatment planning of interventional procedures

Tips and Tricks to optimize Gadovist®-enhanced MRI of vascular disease

Tip one: General protocol recommendations

Gadovist® dose and injection protocol

When CE-MRA is not needed, a Gadovist® dose of 0.1 mmol/kg in combination with GRE sequences is efficacious for perfusion studies (Essig et al. 2013a).

For CE-MRA and DSC (e.g. stroke imaging):

- Double-injection protocol with 2 times 0.05 mmol/kg gadobutrol at 3 mL/sec for the MRA and 5 mL/sec for DSC-MRP with 20 mL saline flush each
- MRA is performed before DSC to avoid influences from circulating contrast media (Essig et al. 2013a)

Field strength

- Minimum 1.5 T
- Higher field strengths (e.g., 3 T) provide superior image quality, if available (Essig et al. 2013b)

Section thickness

- Maximum 5 mm

Target duration of scan

- 20–25 minutes

Tip two: Gadovist®-enhanced MRI: protocol elements for stroke

Standard and Advanced imaging

Recommendations of standard and advanced imaging protocol elements for Gadovist enhanced MRI of stroke are shown in Table 3.1 (Essig et al. 2013a; Wintermark et al. 2008).

Integrated protocols

Consensus is lacking on the optimal protocol for MRI in stroke, but usual sequences include: PWI, DWI, T2-weighted FLAIR imaging, T2*-weighted GRE or SWI, and MRA (Table 6) (Essig et al. 2013a; Wintermark et al. 2008).

Figure 3.1 provides a potential imaging protocol for use in stroke that combines standard and advanced MRI.

Standard	Advanced
T2-weighted FLAIR imaging	MRA (3D TOF, CE-MRA)
DWI	PWI (DSC, DCE)
T2*-weighted GRE and SWI	DWI/PWI

Table 3.1 Elements of imaging protocols for Gadovist®-enhanced MRI of stroke (Essig et al. 2013a; Wintermark et al. 2008)

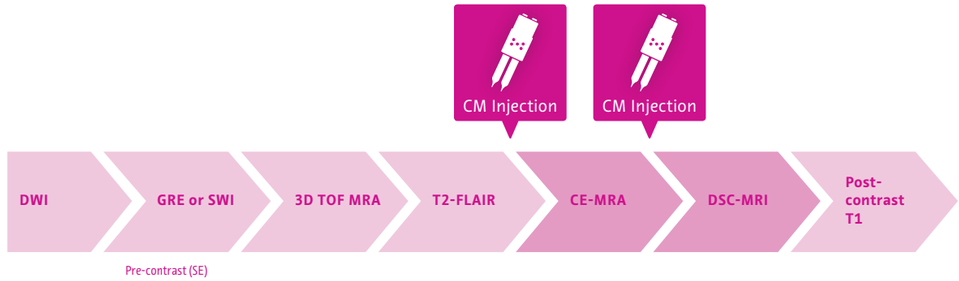

Figure 3.1 Integrated standard and advanced MRI protocol for stroke (Essig et al. 2013b)

Tip three: Gadovist® dosage and injection protocols in MRA

Recommended dosing and injection protocols for cerebral MRA with Gadovist® are shown in Table 3.2.

These values are based on 1.5 T data. To minimize the amount of contrast agent administered, sub-single doses of Gadovist® may be considered if imaging is performed at 3 T (Voth et al. 2009).

For consistency and reproducibility of injection protocols, use of a power injector is highly recommended.

Number of FOVs	<75 kg b.w.	≥75 kg b.w.
1 FOV (corresponding to 0.1–0.15 mmol/kg b.w.)	7.5 mL	10 mL
>1 FOV (corresponding to 0.2–0.3 mmol/kg b.w.)	15 mL	20 mL
Injection protocol	**Gadovist® and saline flow rate**	**Saline volume**
	1.5–2.0 mL/s	20–25 mL

Table 3.2 Recommended dosing and injection protocols for MRA with Gadovist®

Tip four: Optimized image enhancement - matching center of k-space with Gadovist® concentration peak

CE is maximized by matching the central part of k-space with Gadovist® concentration peak (Collins and Scanlon 2012).

The time window for arterial MRA is limited by venous return and varies by vascular region (e.g., 6–9 sec for carotid arteries) (Rummeny et al. 2009). If the center of the k-space correctly matches the contrast peak, venous enhancement data will be present only in the outer part of the k-space and will not interfere with CE (Weishaupt et al. 2006).

Gadovist® offers an optimized, compact bolus geometry due to its double concentration compared with 0.5 M agents.

Injecting this smaller bolus of Gadovist® at the same rate as a 0.5 M agent results in the entire bolus reaching the ROI more rapidly and coherently, with a higher peak concentration (Figure 3.2) (Goyen et al. 2003; Hadizadeh et al. 2014; Herborn et al. 2003).

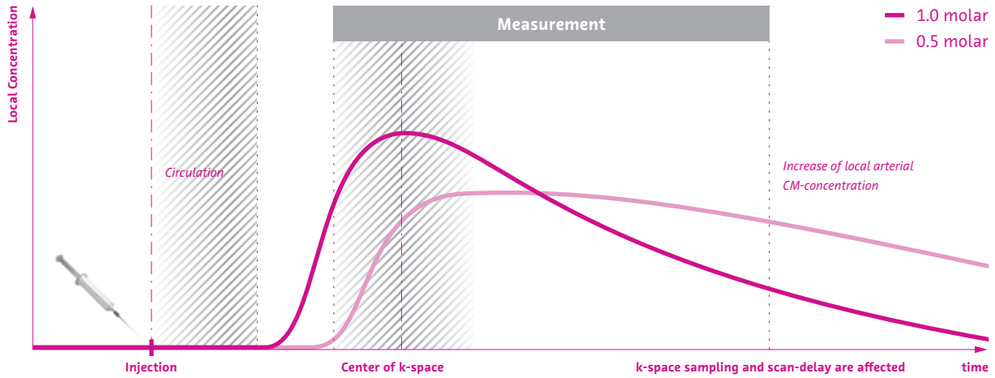

Figure 3.2 Schematic representation of arterial enhancement for 0.5 M and 1.0 M Gd-contrast medium (CM). Scan delay and center of k-space are optimized for 1.0 M CM.

The k-space ordering shown in the drawing is centric, of course other types of ordering can be used with good results, as long as the peak matches the acquisition of the center of k-space.

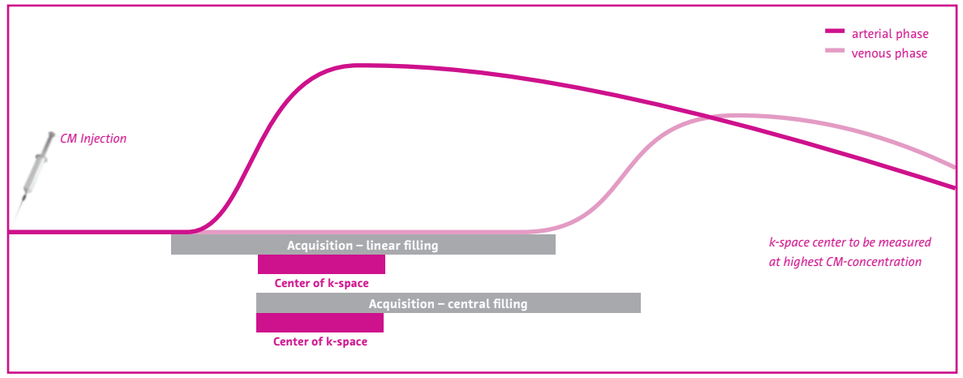

Figure 3.3 For optimal contrast, match the center of k-space with contrast medium (CM) concentration peak. Please note, the two examples of k-space filling match peak enhancement with linear and centric k-space ordering. Notice that the center of k-space is filled at the beginning if centric re-ordering is activated.

Tip five: Maximized image enhancement by optimizing bolus timing

The delay between CM injection and start of data acquisition should be adjusted for each patient to ensure that acquisition of the center of k-space and peak CM concentration coincide Figure 3.3 (Rummeny et al. 2009; Weishaupt et al. 2006).

The time between CM injection and peak concentration in the ROI is dependent upon factors such as injection flow rate and individual patient circulation (Huppertz and Rohrer 2004).

Optimal delay between injection and start of acquisition can be achieved using a bolus timing technique.

Test bolus

A small test bolus of Gadovist®, typically 1 mL, followed by saline flush is injected prior to the examination (Huppertz and Rohrer 2004), and the target area is repeatedly imaged using a fast sequence, e.g., a spoiled T1-weighted 2D GRE sequence, which updates images once every second (Weishaupt et al. 2006). This technique is highly robust but time-consuming, and is only recommended if well-trained personnel are available who have wide experience of performing CE-MRA.

Ensure that the test bolus mimics the injection flow rate and total volume of the later injection. The volume of the test bolus (1 mL) also needs to be replaced by saline volume in the later injection (Huppertz and Rohrer 2004).

Automatic / Semi-automatic techniques

Tools such as SmartPrep by GE Healthcare, BolusTrak by Philips and CARE Bolus by Siemens can assist in detection of bolus arrival and timely initiation of data acquisition. SmartPrep, for example, automatically triggers data acquisition once the signal in a certain ROI has passed a defined threshold. CARE Bolus uses real-time reconstruction to display bolus arrival; once contrast is seen in the vessel of interest, the main sequence can be triggered.

If manual bolus detection and scan initiation is performed, erroneous or delayed sequence initiation is not uncommon (Weishaupt et al. 2006).

Time-resolved MRA (trMRA)

Negates the need for bolus timing –acquisition is initiated directly after injection, and 3D data sets are acquired for each given time period. Due to the high temporal resolution, one data set will coincide with the arrival of the CM bolus (Cornfeld and Mojibian 2009).

trMRA is particularly useful to assess the exact course of blood flow in AVF and vascular malformations (Cornfeld and Mojibian 2009).

Major limitations of this technique are the trade-offs between temporal and spatial resolution and the high post-processing time due to the large number of images (Cornfeld and Mojibian 2009).

Case 6: Carotid Artery Dissection

Vascular disease: stroke and vascular malformations

Patient History

47-year-old female presenting with sudden left head- and neck-pain, followed by right arm paresis and amnestic aphasia. Hours later, sensibility loss and increasing speech disturbance occured. X-ray angiography showed intraluminar thrombus caused by left ACI (A. carotis interna) dissection.

MRI Findings

MR imaging shows a perfusion delay in the left A. cerebri media area, despite regular anastomoses through the A. ophtalmica, A. com. anterior and A. com. posterior. The images depict a pattern of diffusion-failure, caused by both embolus and border infarcts.

Final Diagnosis

Dissection of the left ACI with lack of perfusion.

Patient Outcome

Although the initial MRI shows perfusion delay in the entire left A. cerebri media area, the patient left the hospital with only a distal right hand paresis.

Take-Home Message

Together with DWI, MR perfusion helps to allocate potential ischemic areas in patients with high-grade arterial stenosis or obliteration. Clinical symptoms are still more important than MR-imaging: Watchful waiting can be the method of choice, if the patient is stable. A cath lab team should be on standby.

MR unit		
MR scanner	Siemens Healthcare, Verio	
Operating field strength (T)	3.0	
Coil	TIM Head Coil	
Injection protocol		
Injection system	MEDRAD® Spectris Solaris EP	
	Volume (mL)	**Flow rate (mL/s)**
Gadovist® 1.0	7.5	5
Saline	15	5
Bolus timing technique	Simultaneous start of injection & measurement	
Sequence	**Gadovist® 1.0**	
Sequence	EPI-2D T2*-Perfusion	
Start of scan p.i.	Sim	
Parallel imaging	Grappa 2	
Fat saturation	Yes	
Respiratory state	Free	
TR (ms)	1,500	
TE (ms)	30	
FA (deg)	90	
FOV (mm)	230	
RFOV or Phase FOV (%)	100	
Sequence	**Gadovist® 1.0**	
Matrix	EPI-2D T2*-Perfusion	
Slice orientation	Transversal	
Slice thickness (mm)	4	
Slice gap (mm)	30%	
No. of slices	19	
No. of measurements	50	
Bandwidth (Hz/pixel)	1,446	
k-space ordering	Lin	
Subtraction	No	
Acquisition time (min)	50 × 1.5s = 1:23	

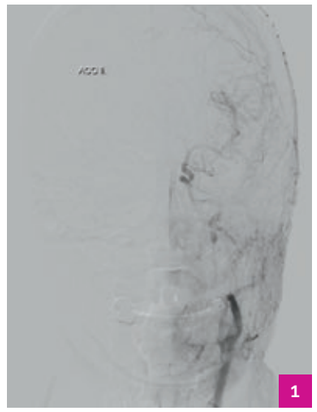

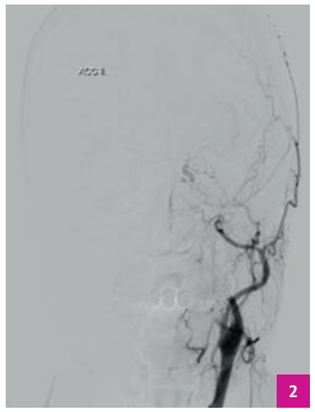

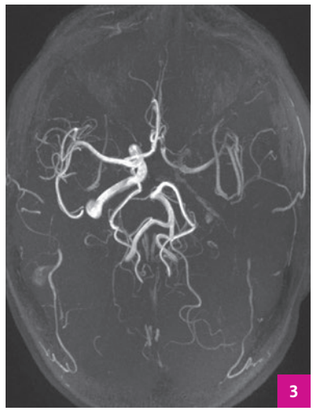

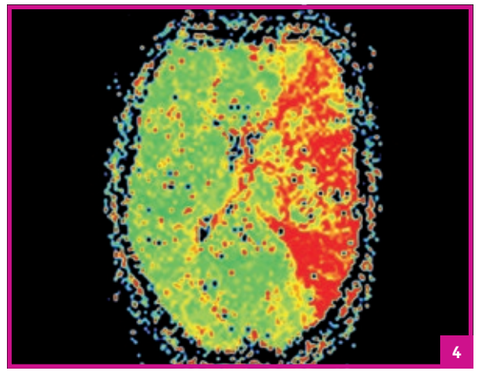

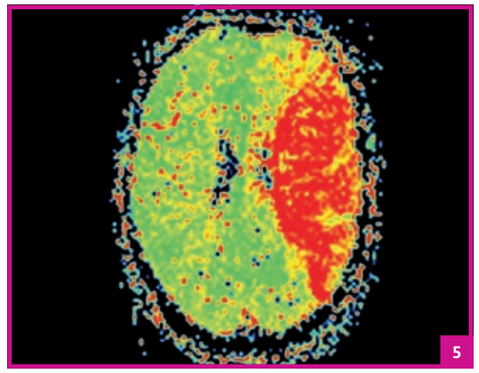

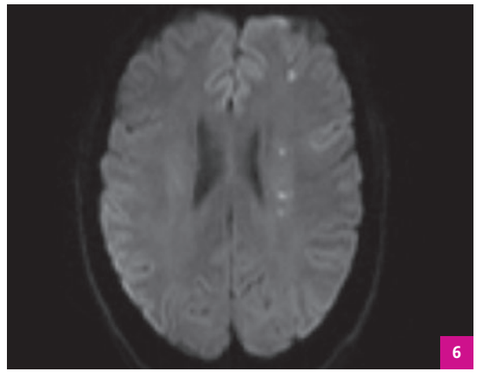

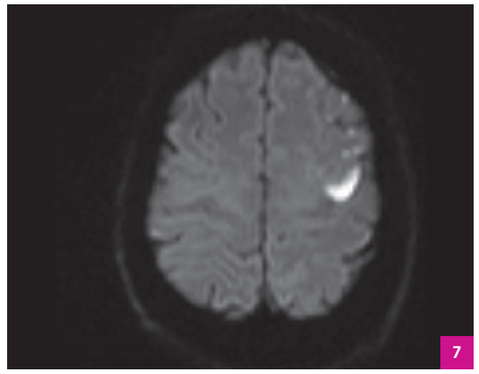

1–2 X-ray Angiography.
3 Time of Flight MRA.
4–5 Perfusion: TTP-Map.
6–7 DWI.

Courtesy of Elke Hattingen,
Johann-Wolfgang-Goethe-University, Frankfurt/Main, Germany

Case 7: Acute Ischemic Stroke

Vascular disease: stroke and vascular malformations

Patient History

75-year-old female, 61 kg, is admitted to the hospital with global aphasia and right hemiplegia. She has a history of arterial hypertension and atrial fibrillation.

She woke up at 8:00 a.m. with right motor weakness and speech disturbance. She was admitted to the hospital with the aphasia and right hemiplegia 45 min later. Her National Institutes of Health Stroke Scale (NIHSS) score at admittance was 15. A brain MR scan was performed 25 min later. Intra-arterial mechanical thrombolysis started at 10:00 a.m.

Take-Home Message

Recent data suggest that multimodal MRI can estimate the potential individual benefit and risk of thrombolysis patients with stroke on awakening. A penumbral pattern on stroke MRI and the lack of signal intensity changes on FLAIR-T2w images indicate patients likely to be within a time window for safe and effective thrombolysis. The following MR features could be used as a marker of the presence of penumbra: MCA occlusion, small diffusion lesion, and substantial PWI-DWI mismatch.

MRI Findings

The contrast-enhanced dynamic susceptibility weighted sequence with a first-pass gadolinium perfusion-weighted technique revealed the extension of the hemodynamic compromise, which is required to determine the presence of DWI-PWI mismatch. This PWI-DWI mismatch, along with the lack of signal-intensity changes on FLAIR, indicated that the patient may still have been within the 6 hours of stroke onset.

Final Diagnosis

Hyperacute ischemic awaking stroke, likely to be within a time window for which thrombolysis could be safe and effective.

Patient Outcome

Thrombolysis resulted in complete recanalization of the left proximal M1 occlusion. The neurologic symptoms regressed rapidly (NIHSS 10 after 2 hours).

MR unit		
MR scanner	Siemens MAGNETOM AVANTO	
Operating field strength (T)	1.5	
Coil	12 Channel Head Coil	
Injection protocol		
Injection system	MEDRAD® Spectris Solaris EP	
	Volume (mL)	**Flow rate (mL /s)**
Gadovist® 1.0	10	2
Saline	10	2
Sequence	**Gadovist® 1.0 DSC**	
Sequence	EPI- 2D SE	
TR (ms)	1,520	
TE (ms)	32	
FA (deg)	90	
FOV (mm)	230	
Matrix	128×128	
Slice thickness (mm)	5	
Acquisition time (min)	1:22	

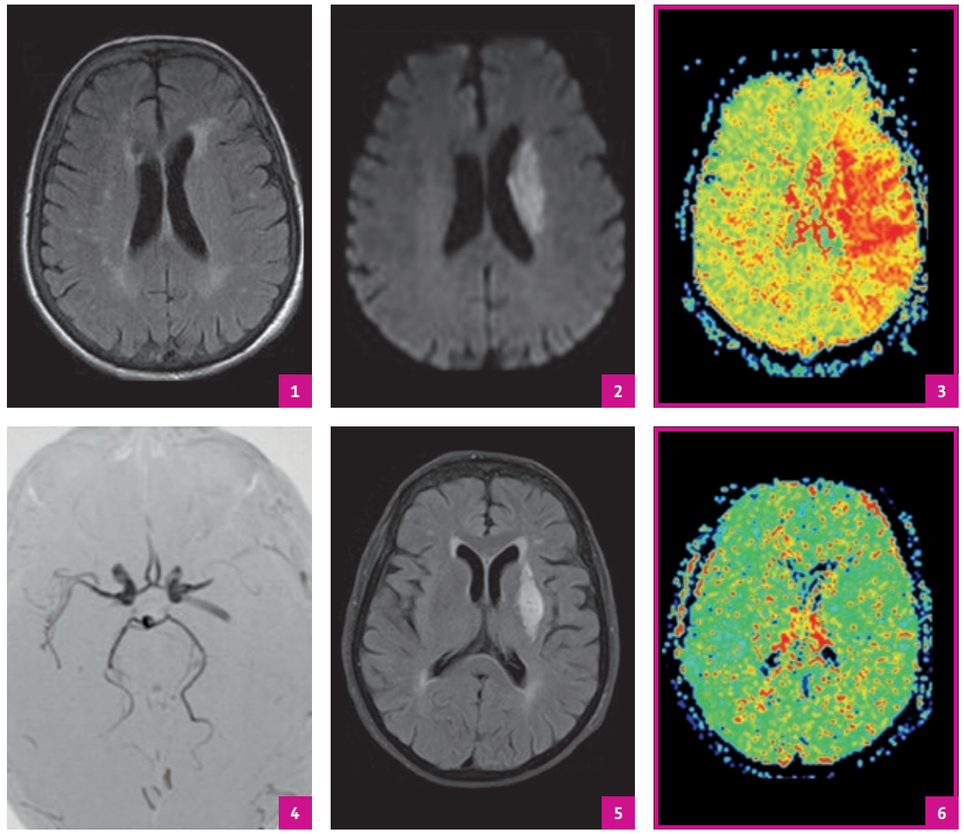

1 T2-FLAIR. No signal abnormalities, suggestive of acute ischemia. No signs of acute ischemia, indicating that the study has been obtained within the first 6 hours after stroke onset.
2 Diffusion-weighted image (EPI-SE). Area of high signal intensity involving the deep territory of the left middle cerebral artery (MCA). Lesion corresponding to acute infarction involving less than one third of the MCA territory.
3 First-pass gadolinium perfusion-weighted imaging (PWI) (echo planar T2* GE). Colored time to peak (TTP) map obtained from the PWI shows prolonged TTP in the deep and superficial MCA territories. Mismatch between the extension of the signal abnormalities identified on the TTP map and on the DWI, indicating ischemic penumbra.
4 3D time-of-flight MR angiography. Maximum intensity projection axial view showing an occlusion of the left A. cerebri media M1 segment. Demonstration of an occluded major intracranial arterial vessel correlating with the ischemic changes identified with DWI, indicating that the patient may benefit from intraarterial recanalization.
5 T2-FLAIR. MRI obtained 24 hours after intraarterial thrombectomy. Acute infarction involving the deep left MCA territory. Lesion matching with the signal abnormality identified on pre-treatment DWI, indicating no lesion growth.
6 First-pass gadolinium perfusion-weighted imaging (PWI) (echo planar T2* GE). Colored time to peak (TTP) map obtained from the PWI showing no asymmetries between brain hemispheres. Normalization of the TTP delay observed in the first MR scan indicates complete recanalization of the MCA territory.

Courtesy of Àlex Rovira,
Hospital universitari Vall d'Hebron, Barcelona, Spain

Inflammatory-Demyelinating Diseases of the CNS: Multiple Sclerosis and Other Variants

Role of CE-MRI

CE-MRI has a major role in the overall diagnostic scheme of multiple sclerosis as well as in selecting patients for immunomodulatory treatment, monitoring disease activity, and predicting treatment response.

Consensus guidelines recommend CE-MRI in every patient with suspected or known MS (Lövblad et al. 2010)

- Contrast enhancement increases the specificity of MS diagnosis, improves patient selection for therapy, and enhances therapeutic follow-up

Applications of CE-MRI in MS include

- Identification of new lesions
- Characterization of lesion activity
- Monitoring disease activity and progression (Lövblad et al. 2010)
- Monitoring and predicting treatment response (Freedman et al. 2013)

McDonald diagnostic criteria

Gadolinium-enhancing lesions clearly indicate active inflammation at the time of the scan, allowing precise discrimination between acute-active from chronic-inactive demyelinating plaques. The last version of the McDonald criteria (McDonald et al. 2001; Polman et al. 2011) allows the demonstration of dissemination in time (one of the requisites to establish the diagnosis of MS), by showing the simultaneous presence of asymptomatic gadolinium-enhancing and non-enhancing lesions (Table 4.1).

This criterion for dissemination in time takes full advantage of the information provided by MR imaging, allowing in some patients a very early diagnosis with one single MR scan obtained at any time interval after symptoms onset.

Three patterns of enhancement have been described in active MS lesions: uniform, ring-like, and open-ring. This last pattern of enhancement is a helpful feature for distinguishing between MS lesions and other focal lesions such as tumors or abscesses (Masdeu et al. 2000).

Higher sensitivity in detecting disease activity can be achieved by adding CE T1W to T2W sequences, as it may be very difficult to identify new lesions based only on T2W sequences especially if they are small, in patients with high lesion load, and when paired scans are obtained with different and poor quality techniques (Freedman et al. 2013). Compared with T2W sequences, CE T1W sequences for detecting disease activity are less subject to the MRI technique used, and are not based on comparison of paired scans.

Applications of Gadovist®-enhanced MRI

- Differential diagnosis
- Identification of new lesion formation – onset of disease and flare-ups
- Monitoring of disease activity and progression, and response to therapy

Lesion characteristic	MRI criterion (based on T2 and CE-T1W sequences)
Dissemination in space	At least 2 of the following: ≥1 juxtacortical lesion ≥1 infratentorial lesion ≥1 periventricular lesion ≥1 spinal cord lesion All lesions in symptomatic regions excluded in brainstem and spinal cord syndromes
Dissemination in time	Simultaneous presence of asymptomatic enhanced and non-enhanced lesions at any time; or A new T2 lesion on follow-up MRI irrespective of timing of baseline scan

Table 4.1 Revised McDonald criteria for diagnosis of MS with CE-MRI (Polman et al. 2011)

Tips and Tricks to optimize Gadovist®-enhanced MRI of inflammatory diseases of the CNS

Tip one: General protocol recommendations

Gadovist® dose

- The standard Gadovist® dose for imaging inflammatory CNS lesions is 0.1 mmol/kg b.w.
- A double dose of Gadovist® (ie, cumulative 0.1 + 0.1 mmol/kg b.w.) increases the sensitivity of CE-MRI to detect acute demyelinating lesions (Rovira et al. 2012)

Field strength

- At least 1.5 T

Section thickness and number

- 3–4 mm slice thickness without gap, covering the whole brain

Image acquisition

- Delay of ≥ 10 min after Gadovist® injection improves the sensitivity of CE-MRI to detect acute demyelinating lesions (Hashemi et al. 2013; Rovira et al. 2012)

Target duration of scan

- 30 min

Tip two: Gadovist®-enhanced MRI: protocol elements

Standard imaging

A simple, standardized protocol for Gadovist®-enhanced MRI is recommended for use across centers (Lövblad et al. 2010). Simple protocols offer time and cost savings relative to more comprehensive protocols, and are likely to diagnose 90% of MS cases. Elements of a standard protocol are shown in Table 4.2.

Advanced imaging

Elements of an advanced protocol are shown in Table 4.2.

Integrated protocols

An integrated sequence for combining standard and advanced protocols for Gadovist®-enhanced MRI is shown in Figure 4.1.

Standard	Advanced
› T2 Dual-echo and FLAIR – axial, whole brain (to detect juxtacortical, periventricular, and posterior fossa lesions)	› Optional DWI (to differentiate other diagnoses, such as acute infarct, or for early detection of treatment related-effects such as progressive multifocal leukoencephalopathy)
› Optional T2-FLAIR – sagittal, midline (to detect corpus callosum lesions). Recommended for initial diagnosis but not required for follow-up studies	› Optional PWI (DSC) to differentiate pseudotumoral MS lesions from tumoral lesions
› Unenhanced T1 (provides little additional information in follow-up studies, but recommended for the initial diagnosis)	
› Contrast-enhanced T1 scan	

Table 4.2 Elements of imaging protocols for Gadovist®-enhanced MRI of MS (Lövblad et al. 2010)

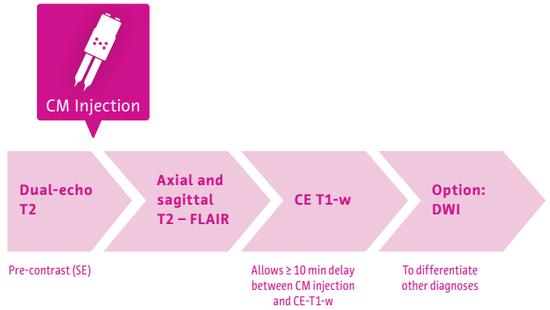

Figure 4.1 Integrated standard and advanced protocol for Gadovist®-enhanced MRI of stroke (Essig et al. 2012)

Case 8: Inflammatory Lesion (MS)

Inflammatory-demyelinating diseases of the CNS

Patient History

47-year-old female with an acute episode of left side motor weakness, presenting with left hemiparesis and an EDSS (expanded disability status scale) of 7 at admission (previous EDSS was 4). Her relapsing multiple sclerosis has been known for 30 years. The patient is now under immunomodulatory treatment with glatiramer acetate. MRI was indicated for the characterization of a new focal lesion (compared to a previous brain MR) located in the right temporal lobe.

MRI Findings

Large necrotic-cystic mass in the posterior subcortical white matter of the right temporal lobe. On the conventional contrast-enhanced T1w sequence, the tumefactive demyelinating lesion (TDL) mimics high grade glioma or metastasis. Dynamic susceptibility contrast MR perfusion sequences show an absence of rCBV increase, which supports the diagnosis of a TDL.

Final Diagnosis

Tumefactive demyelinating lesion.

Patient Outcome

The patient was treated with intravenous methylprednisolone for 5 days that did not provide clinical improvement. Progressive clinical improvement was achieved with five cycles of plasma exchange. A follow up brain MR scan after 1 month demonstrated lesion size decrease and complete disappearance of perilesional edema, supporting the diagnosis of a TDL.

Take-Home Message

Tumefactive demyelinating lesions (TDLs) are a diagnostic challenge. In their acute stage of development, they commonly show peripheral contrast enhancement, perilesional edema and mass effect, mimicking the typical imaging features of high-grade glioma (glioblastoma multiforme). Dynamic susceptibility contrast MR perfusion sequences discriminate active TDLs from high-grade gliomas, based on the analysis of the rCBV. Dynamic susceptibility contrast MR perfusion sequences are helpful in distinguishing TDLs from tumoral or infectious lesions, avoiding unnecessary aggressive therapeutic procedures.

MR unit		
MR scanner	Siemens MAGNETOM TRIO	
Operating field strength (T)	3.0	
Coil	32 Channel Head Coil	
Injection protocol double injection		
Injection system	MEDRAD® Spectris Solaris EP	
	Volume (mL)	**Flow rate (mL/s)**
Gadovist® 1.0	10 (5 + 5)*	5
Saline	15	5
Sequences	**Gadovist® 1.0 DSC**	**Gadovist® 1.0 DCE**
Sequence	T2 EPI-2D fid	T1 2D GRE
TR (ms)	1,450	297
TE (ms)	45	2.46
FA (deg)	90	70
FOV (mm)	230	250
Matrix	128×128	320×256
Slice thickness	5	3
Acquisition time	1:33 min	3:30 min

* 5 mL predose + 5 mL for DSC

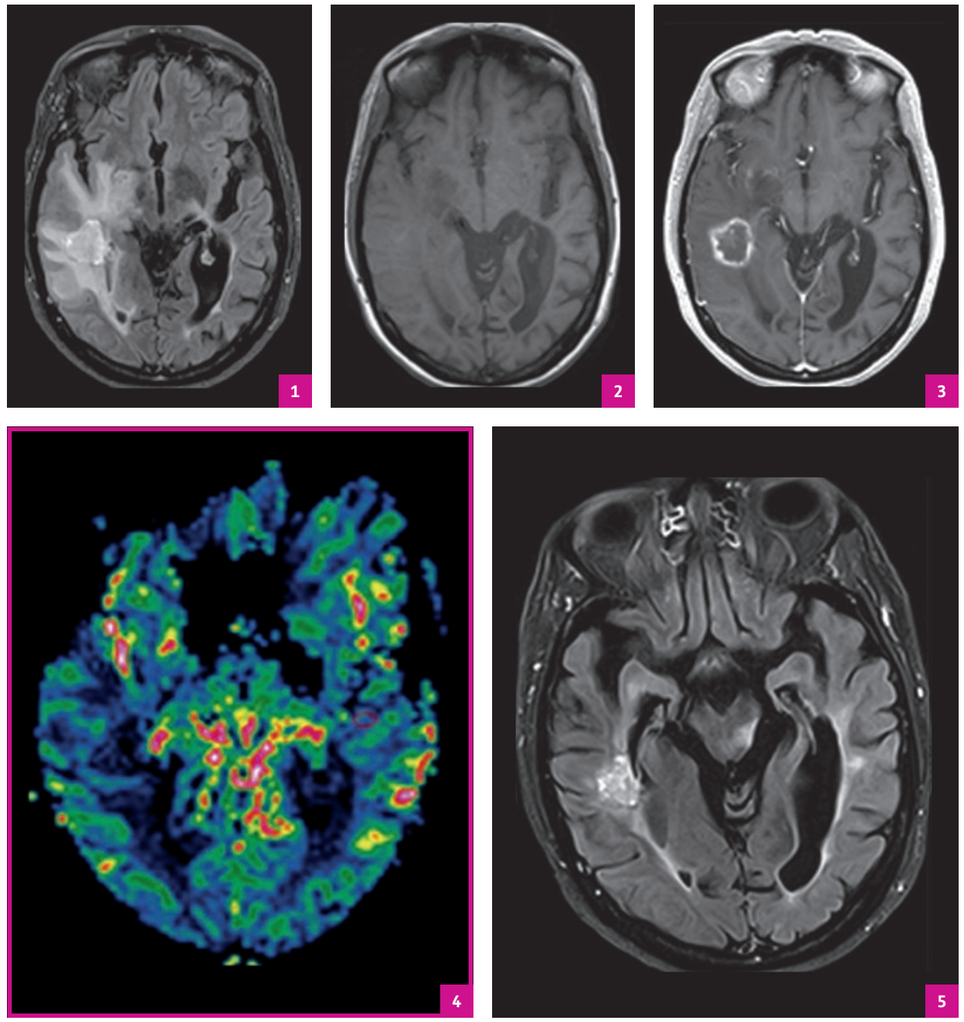

1 T2-FLAIR. Focal well circumscribed lesion in the subcortical right temporal white matter. Extensive edema and mild mass effect. A tumefactive demyelinating lesion is likely, but a malignant tumor cannot be completely excluded.
2–3 Unenhanced T1 SE and contrast-enhanced T1 GE. Focal closed ring-enhancing lesion with irregular margins and central necrosis. Differential diagnosis must include tumefactive demyelinating lesion and a high grade glioma or metastasis.
4 First-pass gadolinium perfusion-weighted imaging (PWI) (echo planar T2* GE). Colored cerebral blood volume (CBV) parametric map obtained from PWI showing no increase in the CBV in enhancing areas of the lesion. No CBV increase in the enhancing part of the lesion, supporting the diagnosis of a tumefactive demyelinating lesion.
5 T2-FLAIR. Follow-up scan performed 1 month later (after treatment). Focal lesion decreased in size, perilesional edema almost disappeared - this supports the diagnosis of a tumefactive demyelinating lesion.

Courtesy of Àlex Rovira,
Hospital universitari Vall d'Hebron, Barcelona, Spain

Neurodegenerative Diseases

Role of CE-MRI

MRI is widely used for assessing neurodegenerative diseases – including Alzheimer's disease, vascular dementia, dementia with Lewy bodies, and Parkinson's disease (Johnson et al. 2012; Román and Pascual 2012; Tuite et al. 2013).

MRI provides information relevant to diagnosis, pathogenesis, disease progression, and treatment response.

Dementias

Standard MRI

Volumetric MRI and cerebrovascular imaging provide precise information on atrophic and vascular changes late in the disease course, valuable in combination with clinical, neuropsychological, and cerebrospinal fluid markers to improve specificity of diagnosis in Alzheimer's disease and vascular dementia (Appel et al. 2009).

Advanced imaging

In the research setting, advanced MR modalities (e.g., DTI, MRS, BOLD fMRI) promise to provide information on white matter involvement preceding neurodegenerative changes (de Souza et al. 2012; Firbank et al. 2007; Mueller et al. 2006; Román and Pascual 2012). Cerebral blood flow can be measured using arterial spin label imaging with potential to differentiate Alzheimer's disease and vascular dementia (Gao et al. 2013).

Parkinson's disease

Standard MRI

T2 and T2* MRI can identify iron deposition in the substantia nigra, as a marker of pathologic change (Schrag et al. 2000; Tuite et al. 2013).

Advanced imaging

SWI provides information on iron deposition and on local tissue geometry, valuable to plan deep brain surgery (Tuite et al. 2013).

Diffusion MRI may provide a differential diagnosis between Parkinson's disease and palsy (Nicoletti et al. 2006; Nicoletti et al. 2008; Seppi et al. 2003).

BOLD fMRI has high temporal and spatial resolution for measuring changes in neural activity in Parkinson's disease, although correlation with clinical changes is unclear (Niethammer et al. 2012).

Applications of Gadovist®-enhanced MRI

Standard MRI

- Detect and quantify degenerative changes/atrophic changes of the brain
- Rule out secondary causes of the patient symptoms, e.g., infections, tumors, metabolic changes
- Rule out CSF circulation changes – e.g., normal pressure hydrocephalus
- Quantify the ischemic components in dementing disorders

Advanced imaging

- Quantify the perfusion changes of the brain parenchyma in neurodegeneration
- Characterize the ischemic components in degenerative diseases
- Rule out acute ischemic changes/components

MRA

- Characterize the hemodynamic components of a degenerative disease – e.g., arteriosclerotic disease components
- Identify vascular malformations that may cause degenerative like symptoms

Tips and Tricks to optimize Gadovist®-enhanced MRI for neurodegenerative disorders of the CNS

Tip one: General protocol recommendations

- T1 GRE 3D volumetric sequences
- SWI to detect amyloid angiopathy
- FLAIR to quantify the ischemic components

Standard imaging

- T1 post contrast in 2D or 3D – or only perform 3D T1 post contrast

Advanced imaging

- DSC-perfusion MRI for assessment of ischemic components

Integrated protocols

- First perform CE-MRA, followed by DSC perfusion MRI

Case 9: Brain Tumor Patient with Clinical Signs of Mental Decline

Neurodegenerative diseases

Patient History

68-year-old female patient, 70 kg, was referred from the Department of Psychiatry with mental decline. An MRI was ordered to rule out secondary causes of dementia. The patient had no pre-existing medical conditions.

MRI Findings

MR images showed a rim enhancing, large frontal tumor with surrounding edema.

Final Diagnosis

Glioblastoma multiforme.

Patient Outcome

The patient had surgery and underwent radiotherapy. Symptoms of dementia completely resolved. Due to tumor progress, the patient underwent chemotherapy.

Take-Home Message

Patients with dementing symptoms or other psychiatric diseases need to undergo an imaging study – due to the better evaluation of morphologic changes MRI is the preferred method. The use of contrast media is not mandatory, however to include perfusion measurements or in cases of pathology the use of CM is needed.

MR unit		
MR scanner	Siemens Magnetom Avanto	
Operating field strength (T)	1.5	
Coil	Head	
Injection protocol		
Injection system	MEDRAD® Spectris Solaris EP	
	Volume (mL)	**Flow rate (mL/s)**
Gadovist® 1.0	7	5
Saline	20	5

Sequences	Native	Native	Native	Gadovist® 1.0	Gadovist® 1.0
Sequence	T1 SE	T2 FSE	FLAIR	T1SE	T1SE / cor
Start of scan p.i. (min)	–	–	–	3	–
Fat saturation	No	No	No	No	No
TR (ms)	750	6,950	8,000	750	600
TE (ms)	20	109	87	20	15
TI (ms)	–	–	2,350	–	–
FA (deg)	90	90	90	90	90
FOV (mm)	230	230	230	230	230
RFOV or Phase FOV (%)	75	75	75	75	75

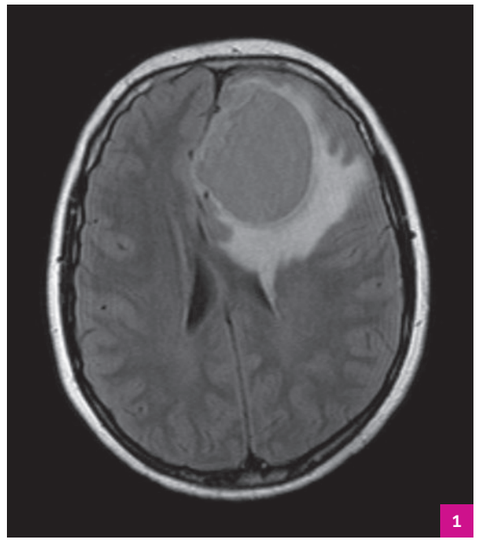

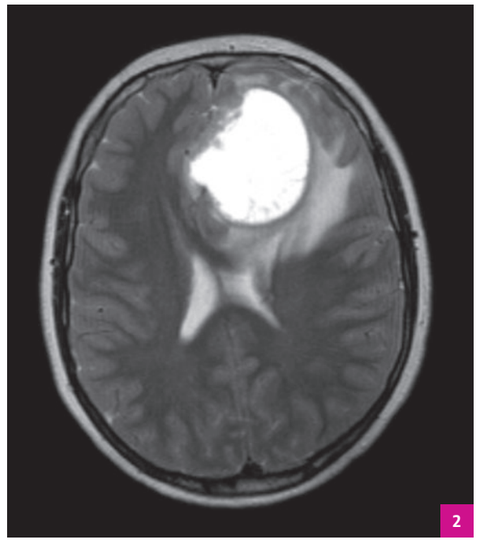

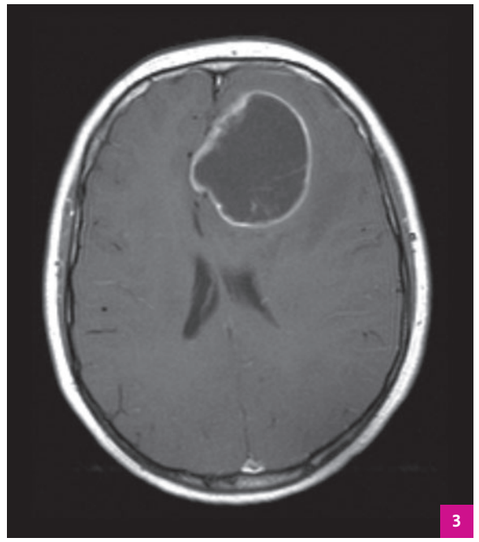

1–3 Large malignant frontal tumor. Rim enhancing and surrounding edema.

Courtesy of Prof. M. Essig,
University of Manitoba , Winnipeg, Canada

Case 10: Alzheimer's Disease with Minor Cognitive Impairment (MCI)

Neurodegenerative diseases

Patient History

70-year-old female, 60 kg, was referred from the Department of Psychiatry with mental decline. An MRI was ordered to rule out secondary causes of dementia. The patient had no pre-existing medical conditions.

MRI Findings

The DSC perfusion MRI in a patient with minor cognitive impairment shows abnormal perfusion on the outlined region of interest (ROI).

Final Diagnosis

No pathology, but abnormal perfusion values.

Patient Outcomes

The patient was diagnosed with suspected Alzheimer's Disease.

Take-Home Message

Patients with dementing symptoms or other psychiatric diseases need to undergo an imaging study – due to the better evaluation of morphologic changes MRI is the preferred method. Compared to normal controls, MR perfusion can identify areas of reduced perfusion in the frontal and temporal areas. The use of contrast media is not mandatory, however, contrast media use is needed to include perfusion measurements or in cases of pathology.

MR unit		
MR scanner	Siemens Magnetom Trio	
Operating field strength (T)	3.0	
Coil	Head	
Injection protocol		
Injection system	MEDRAD® Spectris Solaris EP	
	Volume (mL)	**Flow rate (mL/s)**
Gadovist® 1.0	6	5
Saline	30	5

Sequences	Native	Native	Native	Gadovist® 1.0	Gadovist® 1.0	Gadovist® 1.0
Sequence	T1 SE	T2 FSE	FLAIR	T1SE	T1SE / cor	DSC MRI
Start of scan p.i. (min)	–	–	–	3	–	–
Parallel imaging	–	–	–	–	–	Yes
Fat saturation	No	No	No	No	No	–
TR (ms)	750	6,950	8,000	750	600	1,450
TE (ms)	20	109	87	20	15	45
TI (ms)	–	–	2,350	–	–	–
FA (deg)	90	90	90	90	90	90
FOV (mm)	230	230	230	230	230	230
RFOV or Phase FOV (%)	75	75	75	75	75	–

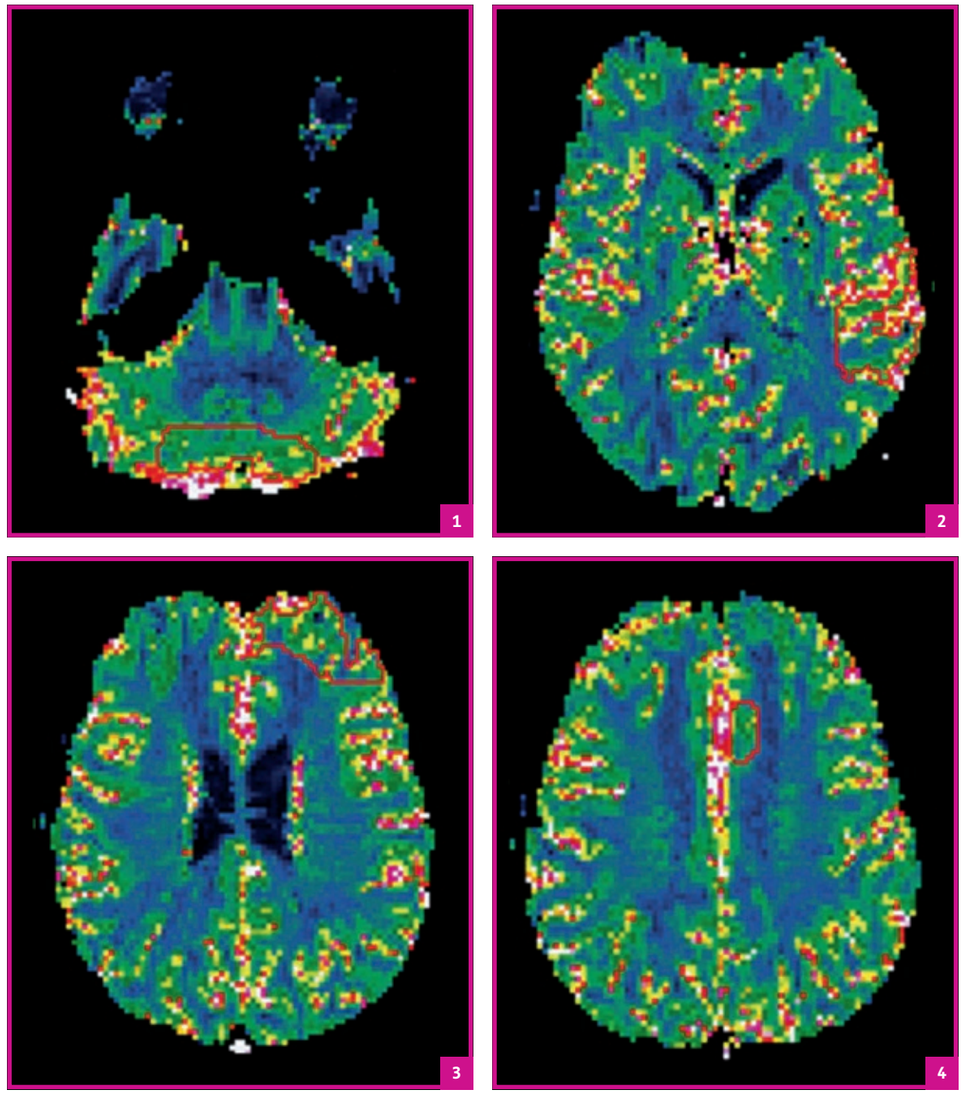

1–4 DSC perfusion MRI – ROI location outlined. Compared to normal controls, MR perfusion identifies areas of reduced perfusion in the frontal and temporal areas.

Courtesy of Marco Essig,
University of Manitoba , Winnipeg, Canada

Infectious Diseases of the CNS

Role of CE-MRI

MRI is superior to CT for evaluation of patients with suspected CNS infections in almost all circumstances

- Relative to CT, MRI offers direct, high-resolution, multiplanar imaging with superior sensitivity for inflammatory change because of its superior demonstration of soft tissue abnormality (Runger 2002; Tunkel et al. 2008)

CE-MRI is mandatory for evaluation of infectious lesions including suspected empyema, ventriculitis, abscess, and encephalitis (Kastrup et al. 2005; Runger 2002)

CE-MRI can also evaluate disease extent and complications such as intracranial herniation, hydrocephalus, subdural or epidural empyema, and venous sinus thrombosis, and assist in biopsy location and treatment planning (Rath et al. Neuroimag Clin N Am 2012)

Contrast-enhanced T2W-FLAIR images have been shown to be superior to contrast-enhanced T1W images in visualization of infectious leptomeningeal disease (Mathews et al. Radiology 1999; Splendiani et al. Neuroradiology 2005)

MRI is more sensitive than CT in the detection of brain abscess because it has greater sensitivity to changes in tissue water content, resulting in greater contrast between edematous brain and normal brain during the early stages of cerebritis and abscess formation (Rath et al. Neuroimag Clin N Am 2012).

MRI features favoring abscess include:

- 2- to 7-mm continuous smooth, thin rim of enhancement
- T2 hypointense rim
- thinning along the medial wall.

However, these features are not consistently present and none are 100% specific (Smirniotopoulos et al. Radiographics 2007). Consequently, attempts have been made to differentiate ring-enhancing neoplasm (glioblastoma, necrotic metastasis) from brain abscess using advanced MRI techniques.

Advanced MRI techniques, including DWI, PWI, 1H-MR spectroscopy and SWI can differentiate infective lesions from tumors (glioblastoma and necrotic brain metastasis) and distinguish infective lesion types at an early stage, allowing prompt institution of appropriate therapy (Kastrup et al. 2005; Rath et al. Neuroimag Clin N Am 2012).

- DWI is helpful in distinguishing ring-enhancing neoplasm from pyogenic abscess. The central non-enhancing portion of a ring-enhancing neoplasm usually demonstrates facilitated diffusion, while restricted diffusion (low ADC) within a ring-enhancing mass is characteristic, but not pathognomonic, of a brain abscess (Kastrup et al. 2005; Hartmann et al. Am J Neuroradiol 2001). Glioblastomas and necrotic brain metastasis may demonstrate low ADC mimicking abscesses (Rath et al. Neuroimag Clin N Am 2012). In short, differentiation of brain abscesses from necrotic glioblastomas with DWI can sometimes be difficult.
- PWI can complement DWI in distinguishing cystic or necrotic ring-enhancing neoplasm from abscess. The mean rCBV of brain tumor walls is higher than that of cerebral abscesses. This difference is attributed to a greater degree of vascularity and blood-brain barrier breakdown in the wall of neoplasm versus the collagenous wall of a mature abscess (Chiang et al. Br J Radiol 2009; Chan et al. Comput Med Imaging Graph 2002).
- 1H-MR spectroscopy can also improve diagnostic confidence in distinguishing cystic or necrotic tumor from abscess (Pal et al. Am J Neuroradiol 2010), since brain abscesses and certain pathogens are characterized by specific resonances that are not present in uninfected tissue.
- Susceptibility-weighted imaging (SWI) may be helpful in differentiating pyogenic abscesses from glioblastomas or brain metastasis. Recent studies have shown that the presence of the dual rim sign is a highly specific feature for abscesses (Toh et al. Am J Neuroradiol 2012; Lai et al. Am J Neuroradiol 2012).

Applications of Gadovist®-enhanced MRI

Standard MRI

- Detect infectious diseases – meningeal and parenchymal abnormalities
- Differential diagnosis, e.g., tumors and abscesses
- Define spread of disease
- Characterize secondary changes related to infections, e.g., hydrocephalus, venous sinus thrombosis, intracranial herniation, subdural or epidural empyema.

Advanced MRI

- Complement conventional MR imaging.
- Improve diagnostic confidence in distinguishing cystic or necrotic tumor from abscess based on structural, hemodynamic, and metabolic differences between these two types of lesions

Tips and Tricks to optimize Gadovist®-enhanced MRI for infectious diseases

Tip one: General protocol recommendations

- Pre and post contrast images in different planes

Tip two: Gadovist®-enhanced MRI of infectious diseases of CNS: protocol elements

Recommended standard and advanced protocol elements for Gadovist®-enhanced MRI of infectious diseases of the CNS are shown in Table 6.1. An integrated protocol is illustrated in Figure 6.1

Standard	Advanced
Pre and CE-T1W Axial and sagittal pre- and post-contrast T1W images	PWI
Axial T2W images	MRS
Coronal post-contrast T1W images	SWI
Post-contrast axial T2W FLAIR images	
DWI	

Table 6.1 Elements of imaging protocols for Gadovist®-enhanced MRI of infectious diseases of the CNS

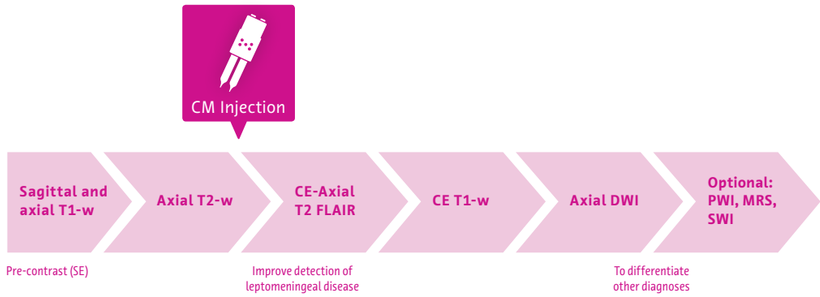

Figure 6.1 Integrated standard and advanced protocol for Gadovist®-enhanced MRI of infectious disease of the CNS

Case 11: Cerebral Abscess

Infectious diseases of the CNS

Patient History

47-year-old man, presenting with gait disturbance, followed by generalized epileptic seizures. Pre-existing polytoxicomania (drugs, alcohol) and hepatitis. A prior CT showed multiple space-occupying lesions.

MRI Findings

MR images showed seven intraparenchymal lesions with diameters up to 3.6 cm, showing restricted diffusion in DWI, extensive edema in T2 and rim enhancement after Gd.

Final Diagnosis

Multiple cerebral abscesses, caused by the Streptococcus milleri group (biopsy-proven).

Take-Home Message

As there is a wide range of differential diagnoses for rim-enhancing lesions, DWI is mandatory in the workup of suspected encephalitis/abscess.

MR unit		
MR scanner	Siemens Verio, VQ engine	
Operating field strength (T)	3.0	
Coil	32 Channel Head Coil	
Injection protocol		
Injection system	Manual	
	Volume (mL)	**Flow rate (mL/s)**
Gadovist® 1.0	8	~ 1
Saline	–	–

Sequence(s)	Native	Native	Gadovist® 1.0
Sequence	DWI	T2	T1 MPR
Fat saturation	No	No	Yes
Respiratory state	Free	Free	Free
TR (ms)	3,500	5,000	–
TE (ms)	89	95	–
FA (deg)	90	150	–
FOV (mm)	230	192×220	256×256
RFOV or Phase FOV (%)	100	87.5	100
Matrix	128×128	512×269	256×256
Slice orientation	Axial	Axial	Axial
Slice thickness (mm)	4	1	1
Slice gap (mm)	1.2	1	0
No. of slices	25 (b=0 and b=1000 each)	24	180 (reformatted)
No. of measurements	4	1	–
Bandwidth (Hz/pixel)	1,260	184	–
Subtraction	No	No	–

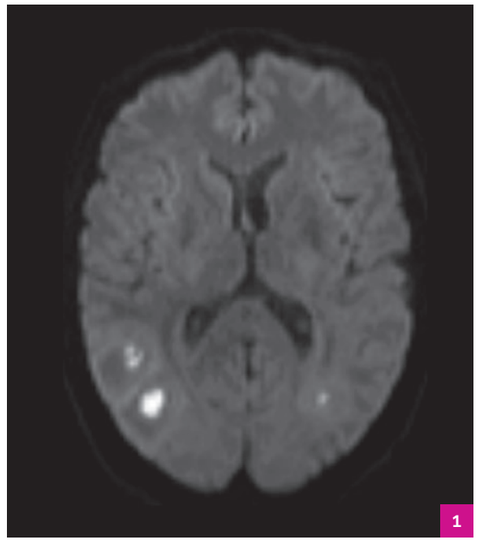

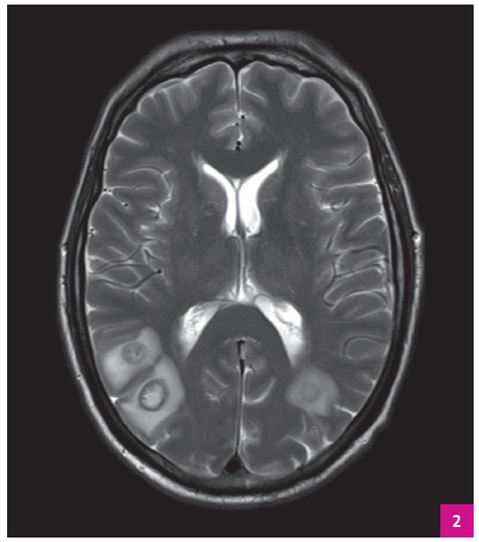

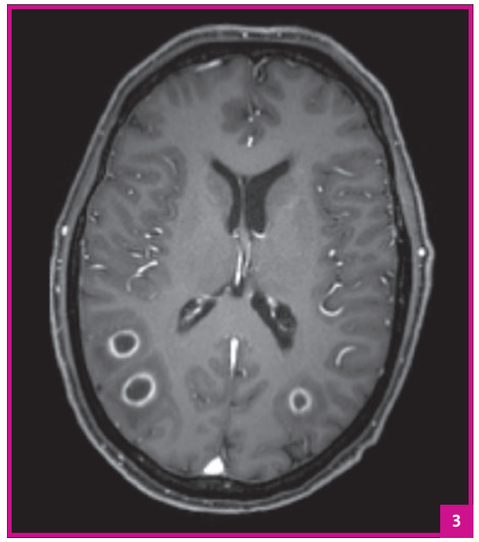

1–3 Seven intraparenchymal lesions with diameters up to 3.6 cm. Restricted diffusion in DWI. Extensive edema in T2 and rim enhancement after Gd.

Courtesy of Christoph Ozdoba,
Inselspital, University of Bern, Switzerland

Case 12: Tuberculous Meningitis

Infectious diseases of the CNS

Patient History

35-year-old female with previous tuberculous meningitis, now presenting for follow-up examination. The second study is performed 6 weeks after the start of combination therapy.

MRI Findings

MR images of the first study predominantly show subarachnoid enhancement with granulomatous nodules. In the second study, after six weeks of therapy, a marked lesion load decrease and lower enhancement can be found.

Final Diagnosis

Tuberculous meningitis/arachnoiditis with typical nodules.

Take-Home Message

For follow-up in therapy control, try to reproduce the original study as closely as possible (slice position and thickness, sequences).

MR unit and coils		
MR scanner	Siemens Verio, VQ engine	
Operating field strength (T)	3.0	
Coil	32 Channel Head Coil	
Injection protocol		
Injection system	Manual	
	Volume (mL)	**Flow rate (mL/s)**
Gadovist® 1.0	7.5	~ 1
Saline	–	–

Sequences	Native	Native	Gadovist® 1.0
Sequence	DWI	T2	T1 3D
Fat saturation	No	No	Yes
Respiratory state	Free	Free	Free
TR (ms)	3,500	3,760	–
TE (ms)	89	85	Reformatted Images
FA (deg)	90	150	–
FOV (mm)	230×230	192×220	256
RFOV or Phase FOV (%)	100	87.5	–
Matrix	128×128	269×512	256×256
Slice orientation	Axial	Axial	Axial
Slice thickness (mm)	4	5	1
Slice gap (mm)	1.2	1	0
No. of slices	25 (each for b=0 and b=1,000)	24	1st study 238 2nd study 226
No. of measurements	4	1	–
Bandwidth (Hz/pixel)	1,260	184	–
Subtraction	No	No	No

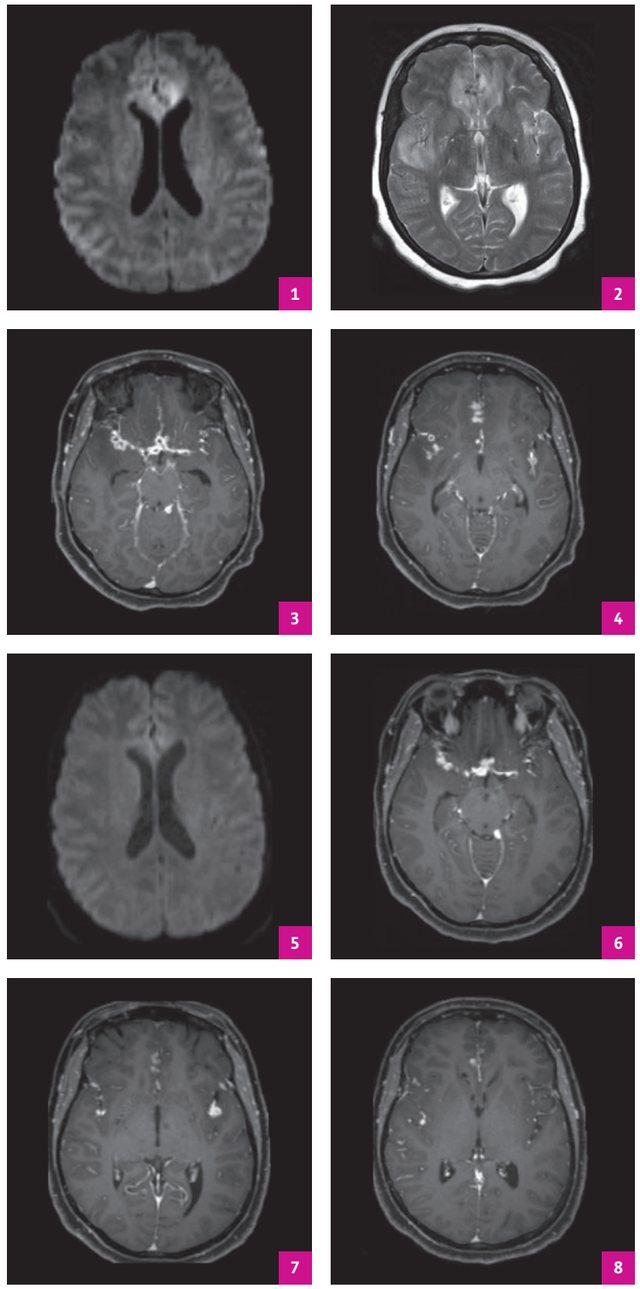

1–4 Predominantly subarachnoid enhancement with granulomatous nodules.
5–8 Marked decrease of lesion load and enhancement after six weeks of therapy.

Courtesy of Christoph Ozdoba, University of Bern, Inselspital, Switzerland

Characteristics of Gadovist®

Gadovist® enhancement for MRI and MRA in CNS imaging

Gadovist® is an extracellular contrast agent approved for standard CE-MRI of all body regions* including brain and spine, head and neck region, lung, breast, abdomen, pelvis, kidney, extremities and musculoskeletal system, as well as cardiac MRI to diagnose coronary heart disease, in adults, adolescents and children of all ages including term neonates.

Gadovist® is also approved for CE-MRA in adults, adolescents, and children of all ages (Gadovist® Summary of Product Characteristics). Gadovist®-enhanced MRA enables spatially (3D) and temporally (4D) resolved depiction of the cerebral vasculature, allowing 3D visualization of the vessel network and tracking of blood flow over time.

Properties of Gadovist®

Gadovist® is a unique extracellular contrast agent that offers:

- Double gadolinium concentration (1 M), which requires half the injection volume compared with other (0.5 M) GBCAs
- High relaxivity (Huppertz and Rohrer 2004)
- High T1-shortening per volume (Port et al. 2005; Rohrer et al. 2005)
- Similar osmolality and viscosity relative to other (0.5 M) GBCAs (Vogler et al. 1995)
- Improved image quality in standard MRI, proven in clinical trials (reported in later sections of this brochure)
- In an animal model, it could be demonstrated that a substantially lower amount of Gadovist® (0.1 mmol/kg b.w.) was needed to reach the same efficacy as a 0.5 M GBCA (gadoterate meglumine, at 0.15 mmol/kg b.w.), which may be beneficial for patients with impaired renal function. In addition, increasing the dose of Gadovist® to 0.15 mmol/kg b.w. can potentially lead to better delineation of lesions (Kramer et al. 2010)
- Smaller bolus width, smaller mean peak time, higher contrast, and higher CNR relative to GBCAs with 0.5 mol/L formulations in advanced imaging (Essig et al. 2013b; Tombach et al. 2003)
- Optimal signal enhancement observed during arterial first pass for CE-MRA within a period of about 15 min after injection (Gadovist® 2013)
- High chelate stability class due to macrocyclic structure (American College of Radiology 2010; European Medicines Agency 2009; Frenzel et al. 2008; Thomsen et al. 2013)
- Proven safety and tolerability, including in renally impaired patients (Tombach and Heindel 2002; Voth et al. 2011)

Overview of dosing/protocols for Gadovist®-enhanced MRI and MRA

- Approved doses of Gadovist® for MRI of the CNS are 0.1 mmol/kg (up to 0.3 mmol/kg b.w.) in adults and 0.1 mmol/kg b.w. in children including term neonates (see dosing details in Appendixes 1 and 2)
- Most CNS lesions can be detected using the standard Gadovist® dose of 0.1 mmol/kg b.w. Additional doses up to 0.3 mmol/kg b.w. in adults may be advantageous in cases of diagnostic doubt (except for patients with severe renal impairment) (Essig et al. 2012)
- The Gadovist® dose for CE-MRA is 7.5 mL or 10 mL with b.w. <75 kg or ≥75 kg, respectively, for 1 FOV; and 15 mL or 20 mL with b.w. <75 kg or ≥75 kg, respectively, for >1 FOV (Appendix 3)
- Gadovist® is administered intravenously as a bolus injection either manually or by power injector

Benefits of Gadovist® – Selected Study Evidence on CE Neuroimaging Protocols

Primary and metastatic tumors of the brain and spine

Standard MRI

Lesion localization, identification, delineation, and characterization

- Use of Gadovist®-enhanced MRI provides clinical benefits versus gadopentetate, gadoterate, and gadoteridol at the same dose for lesion localization, identification, and in contrast enhancement characteristics in primary and secondary brain tumours. (Anzalone et al. 2009; Anzalone et al. 2013b; Gutierrez et al. 2014; Kim et al. 2010; König et al. 2013; Maravilla et al. 2014)
- Gadovist® (0.1 mmol Gd/kg b.w.) is equivalent to gadoteridol at double dose (0.2 mmol Gd/kg b.w.) for detecting brain metastases (Katakami et al. 2011)

Guidance on therapy and post therapeutic response assessment

- Gadovist®-enhanced MRI offers significant benefits in treatment planning, including selection of SRS for metastases based on lesion number and location (Anzalone et al. 2009; Anzalone et al. 2013b; Kim et al. 2010)

Advanced imaging

Lesion localization, identification, delineation, and characterization

- Gadovist®, because of its double gadolinium concentration, offers the practical advantage of a smaller injection volume, especially in high-dose applications, which provides a more compact and "sharper" bolus (Huppertz and Rohrer 2004; Tombach et al. 2003)
- Gadovist® is significantly superior to gadopentetate for delineation between gray and white matter and demarcation of highly vascularized tumor tissue (Giesel et al. 2009)

Vascular disease: stroke and arteriovenous malformations

Stroke

Advanced imaging

Identification and grading of ischemic events and progression over time

- Gadovist® at a dose of 0.1 mmol/kg provides high-quality, diagnostically valid perfusion maps in cerebral PWI (Essig et al. 2006)

MRA

Visualization of vascular anatomy and vessel stenosis

- Gadovist®-enhanced MRA facilitates the diagnosis of ischemic stroke by accentuating abnormal flow kinetics and the diagnosis of non-ischemic stroke by assisting the detection and characterization of intracranial aneurysms and AVMs. Gadovist® may also be employed to characterize vascular atherosclerotic plaque (Essig and Tanenbaum 2013)
- Gadovist®-enhanced MRA combined with duplex sonography provides accurate grading of stenoses of the internal carotid artery (Lee et al. 2011)
- Gadovist®-enhanced MRA aids characterization of aneurysmal remnants after coiling, including contrast filling within the coil mass (Agid et al. 2008) and in the presence of a stent (Agid et al. 2012)
- Gadovist®-enhanced MRA demonstrates high signal and contrast for evaluation of carotid and supraaortic arteries (Kramer et al. 2011; Kramer et al. 2013)
- May be an alternative to DSA for screening and surveillance of dural AVF (Farb et al. 2009)
- Gadovist®-enhanced MRA reliably assesses AVMs pre- and postoperatively (Hadizadeh et al. 2012; Kukuk et al. 2010)
- More accurate estimation of neck vessel stenosis due to more compact bolus than 0.5 M agents (Engelhorn and Doerfler 2008)

Inflammatory diseases of the CNS: multiple sclerosis and other applications

Identification of new lesion formation and monitoring of disease activity

- By providing information on new lesion formation, Gadovist®-enhanced MRI:
  - Aids early diagnosis of disease, allowing earlier initiation of treatment
  - Offers insights into pathogenesis, by identifying correlations with various markers of immune system activation and showing the pivotal role of breaching the blood-brain barrier
  - Allows monitoring of response in individual patients to first-line disease-modifying therapies such as Betaferon®/Betaseron®
  - Provides an efficacy outcome in trials of novel disease-modifying therapies (Filippi and Rocca 2011; Lövblad et al. 2010)

The high relaxivity provided by Gadovist® results in increased lesion enhancement (Lövblad et al. 2010).

Lesion enhancement is increased by introducing a delay of 15 min after Gadovist® injection. This delay increases lesion detection rates (Lövblad 2008; Rovira et al. 2012; Uysal et al. 2007).

The benefits of Gadovist® have now been documented in the most relevant areas of CNS imaging. New studies are ongoing in additional areas, including neurodegenerative diseases.

Appendix I: Glossary

Abbreviation	Definition	Description
ADC	apparent diffusion coefficient	A measure of the magnitude of diffusion (of water molecules) within cerebral tissue. A high ADC value indicates that cortical white matter tracts are disorganized. ADC is calculated from DWI (see below).
ASL	arterial spin labeling	A technique that uses water in arterial blood as an endogenous contrast agent, by marking a specific vessel with a radiofrequency pulse. By subtracting images with/without markings, observations can be made about relative blood flow.
AVM	arteriovenous malformation	-
AVF	arteriovenous fistula	-
b.w.	body weight	-
CE	contrast enhancement	The improved tissue contrast provided by contrast agents such as GBCAs.
CNR	contrast-to-noise ratio	The difference in signal-to-noise (SNR) ratios between two tissue types, A and B. CNR = SNR(A) – SNR(B) / standard deviation.
CT	computed tomography	-
CTA	computed tomographic angiography	-
DCE	dynamic contrast-enhanced	A technique involving acquisition of serial T1-weighted images before, during, and after administration of extracellular low-molecular-weight MR contrast media, such as a GBCA. The resulting signal intensity–time curve reflects a composite of tissue perfusion, vessel permeability, and extravascular-extracellular space.
DSA	digital subtraction angiography	
DSC	dynamic susceptibility contrast	A technique in which the first pass of a bolus of GBCA through brain tissue is monitored by a series of T2- or T2*-weighted MR images. Also known as perfusion-weighted imaging (PWI).
DTI	diffusion tensor imaging	MRI technique for displaying the directional dependency of diffusion. Applications include assessment of the architecture, configuration and integrity of nerve fiber bundles.
DWI	diffusion-weighted imaging	MRI technique sensitive to diffusive movements in tissue. Diffusion movements reduce signal. A reduction in diffusion means the reduction in signal is less intense. As a result, affected regions are displayed brighter.
ETL	echo train length	The length of two or more echoes in sequence, each of them obtaining a different phase-encoding direction.
FA	flip angle	The angle to which net magnetization is rotated relative to the main magnetic field direction via application of radiofrequency pulse.
FFE	fast field echo/field echo	The echo produced by reversing the direction of the magnetic field gradient to cancel out the position-dependent phase shifts that accumulated due to the gradient.
FLAIR	fluid-attenuated inversion recovery	Sequences to suppress the signals generated by fluids in the body. FLAIR produces strong T2 weighting, suppresses CSF signal, and minimizes contrast between gray matter and white matter, to produce enhanced lesion visibility.
FOV	field of view	The spatial area of the image (in 2 or 3 dimensions) that contains the object of interest. For the same matrix size, the smaller the field of view, the higher is the resolution (smaller voxels).
FSE	fast spin echo	The basic 90°-180° spin echo excitation plus multiple 180° refocusing pulses.
GBCA	gadolinium-based contrast agent	Agent that enhances the signal intensity of tissues by shortening relaxation times.
Gd	gadolinium	Paramagnetic ion utilized in GBCA. Administered in chelated form (linear or macrocyclic) to reduce toxicity.
GRE	gradient recalled echo	Sequence using gradients to rephase the protons and create the echo.
IV	intravenous	-
MRA	magnetic resonance angiography	-
MRI	magnetic resonance imaging	-
MRS	magnetic resonance spectroscopy	A technique that measures the MR spectrum in a tissue to provide information on metabolism. The brain metabolites commonly seen on the MR spectrum are N-acetylaspartate (NAA), a neuronal marker; choline-containing compounds (Cho), a marker of membrane turnover; and creatine-phosphocreatine (Cr); as well as the presence of lipids and lactate.
MS	multiple sclerosis	–
MSD	mean square difference	-

MT	**magnetization transfer**	Sequence used to decrease signal from certain tissues, e.g., used as background signal suppression in MRA. A selective saturation pulse suppresses the signal from protons bound in molecules; through proton exchange with the surrounding free proton pool, some of the loosely bound protons reach the free proton pool and transfer the magnetization to the free protons. This in turn decreases the signal from the free proton pool.
MTT	**mean transit time**	The ratio of cerebral blood volume to cerebral blood flow (CBV/CBF) – used as an indicator of the cerebral circulation in perfusion MRI.
NCE-MRA	**non-contrast enhanced magnetic resonance angiography**	-
NEX	**number of excitations**	The average number of times that each line of k-space data is acquired during an MRI scan.
PET	**positron-emission tomography**	-
PWI	**perfusion-weighted imaging**	See DSC.
rCBF	**relative cerebral blood flow**	CBF: A perfusion parameter representing the blood flow per unit time through a region of brain.
rCBV	**relative cerebral blood volume**	CBV: A perfusion parameter representing the volume of blood in a given volume of brain tissue. rCBV: The ratio or difference between a ROI (region of interest) in the abnormal area and in an area (e.g., contralateral, mirror ROI) considered to be a normal reference.
SRS	**stereotactic radiosurgery**	-
SWI	**susceptibility-weighted imaging**	MRI technique that displays abnormal vascular changes via localized changes in magnetic fields, caused by deoxygenated blood or local iron deposits.

TE	**echo delay time**	The time between the excitation pulse of a sequence and the resulting echo used as the MR signal.
TI	**inversion time**	The time period between the 180° inversion pulse and the subsequent 90° excitation pulse in an inversion recovery pulse sequence.
TIA	**transient ischemic attack**	-
TOF	**time of flight**	An MRA technique that relies on flow of unsaturated blood into a magnetized presaturated slice. The difference between unsaturated and presaturated spins creates a bright vascular image.
TR	**relaxation time**	After excitation, transverse magnetization decays toward zero with a characteristic time constant T2, and longitudinal magnetization returns toward equilibrium with a characteristic time constant T1.
TSE	**turbo spin echo**	A fast multi-echo sequence, in which each echo of a pulse train includes a different phase encoding. The turbo factor increases speed, and is frequently used to improve resolution.
TTP	**time to peak**	The time from the beginning of contrast material injection to the maximum concentration of contrast material in a region of interest.
WBRT	**whole brain radiotherapy**	-

Appendix II: References

Agid R, Schaaf M, Farb R. CE-MRA for follow-up of aneurysms post stent-assisted coiling. *Interv Neuroradiol.* 2012;18(3):275-283.

Agid R, Willinsky RA, Lee SK, et al. Characterization of aneurysm remnants after endovascular treatment: contrast-enhanced MR angiography versus catheter digital subtraction angiography. *Am J Neuroradiol.* 2008;29(8):1570-1574.

Alfke K, Jensen U, Pool C, et al. Contrast-enhanced magnetic resonance angiography in stroke diagnostics: additional information compared with time-of-flight magnetic resonance angiography? *Clin Neuroradiol.* 2011;21(1):5-10.

American College of Radiology. ACR Committee on Drugs and Contrast Media: ACR guidelines on Nephrogenic Systemic Fibrosis. American College of Radiology. http://www.acr.org/SecondaryMainMenuCategories/quality_safety/contrast_manual/NephrogenicSystemicFibrosis.aspx. Accessed January 22, 2014.

Anzalone N. Comparative studies of different gadolinium agents in brain tumors: differences between gadolinium chelates and their possible influence on imaging features. *Am J Neuroradiol.* 2010;31(6):981-982.

Anzalone N, Essig M, Lee SK, et al. Optimizing contrast-enhanced magnetic resonance imaging characterization of brain metastases: relevance to stereotactic radiosurgery. *Neurosurgery.* 2013a;72(5):691-701.

Anzalone N, Gerevini S, Scotti R, et al. Detection of cerebral metastases on magnetic resonance imaging: intraindividual comparison of gadobutrol with gadopentetate dimeglumine. *Acta Radiol.* 2009;50(8):933-940.

Anzalone N, Scarabino T, Venturi C, et al. Cerebral neoplastic enhancing lesions: multicenter, randomized, crossover intraindividual comparison between gadobutrol (1.0M) and gadoterate meglumine (0.5M) at 0.1 mmol Gd/kg body weight in a clinical setting. *Eur J Radiol.* 2013b;82(1):139-145.

Appel J, Potter E, Shen Q, et al. A comparative analysis of structural brain MRI in the diagnosis of Alzheimer's disease. *Behav Neurol.* 2009;21(1):13-19.

Bauknecht HC, Romano VC, Rogalla P, et al. Intra- and interobserver variability of linear and volumetric measurements of brain metastases using contrast-enhanced magnetic resonance imaging. *Invest Radiol.* 2010;45(1):49-56.

Breuer J, Gutierrez J, Latchaw R, et al. Gadobutrol in the central nervous system at three doses: Results from a phase II, randomized, multicenter trial. *J Magn Reson Imaging.* 2013;39:410-418.

Byrnes KR, Ross CB. The current role of carotid duplex ultrasonography in the management of carotid atherosclerosis: foundations and advances. *Int J Vasc Med.* 2012;2012:187872.

Clevert DA, Johnson T, Michaely H, et al. High-grade stenoses of the internal carotid artery: comparison of high-resolution contrast enhanced 3D MRA, duplex sonography and power Doppler imaging. *Eur J Radiol.* 2006;60(3):379-386.

Collins JD, Scanlon T. Lower extremity peripheral arterial disease. *Magnetic Resonance Angiography: Principles and Applications.* New York, NY: Springer; 2012:319-322.

Cornfeld D, Mojibian H. Clinical uses of time-resolved imaging in the body and peripheral vascular system. *Am J Roentgenol.* 2009;193(6):W546-W557.

de Souza LC, Lehericy S, Dubois B, et al. Neuroimaging in dementias. *Curr Opin Psychiatry.* 2012;25(6):473-479.

Duong TQ, Fisher M. Applications of diffusion/perfusion magnetic resonance imaging in experimental and clinical aspects of stroke. *Curr Atheroscler Rep.* 2004;6(4):267-273.

Elster AD, King JC, Mathews VP, et al. Cranial tissues: appearance at gadolinium-enhanced and nonenhanced MR imaging with magnetization transfer contrast. *Radiology.* 1994;190(2):541-546.

Engelhorn T, Doerfler A. High-molar contrast agents for CNS application. *Imaging Decisions MRI.* 2008;11(4):26-32.

Essig M, Anzalone N, Combs SE, et al. MR imaging of neoplastic central nervous system lesions: review and recommendations for current practice. *Am J Neuroradiol.* 2012;33(5):803-817.

Essig M, Giesel F, Le-Huu M, et al. Perfusion MRI in CNS disease: current concepts. *Neuroradiology.* 2004;46 Suppl 2:s201-s207.

Essig M, Lodemann KP, Le-Huu M, et al. Intraindividual comparison of gadobenate dimeglumine and gadobutrol for cerebral magnetic resonance perfusion imaging at 1.5 T. *Invest Radiol.* 2006;41(3):256-263.

Essig M, Nguyen TB, Shiroishi MS, et al. Perfusion MRI: the five most frequently asked clinical questions. *Am J Roentgenol.* 2013a;201(3):W495-W510.

Essig M, Shiroishi MS, Nguyen TB, et al. Perfusion MRI: the five most frequently asked technical questions. *Am J Roentgenol.* 2013b;200(1):24-34.

Essig M, Tanenbaum L. Magnetic resonance imaging techniques in the evaluation of stroke and neurovascular disease. *Eur Neurol Rev.* 2013;8:14-20.

European Medicines Agency. European Medicines Agency makes recommendations to minimise risk of nephrogenic systemic fibrosis with gadolinium-containing contrast agents. European Medicines Agency. http://www.ema.europa.eu/ema/index.jsp?curl=pages/news_and_events/news/2009/11/news_detail_000408.jsp&mid=WC0b01ac058004d5c1. Accessed January 22, 2014.

Farb RI, Agid R, Willinsky RA, et al. Cranial dural arteriovenous fistula: diagnosis and classification with time-resolved MR angiography at 3T. *Am J Neuroradiol.* 2009;30(8):1546-1551.

Fiebach JB, Schellinger PD, Jansen O, et al. CT and diffusion-weighted MR imaging in randomized order: diffusion-weighted imaging results in higher accuracy and lower interrater variability in the diagnosis of hyperacute ischemic stroke. *Stroke.* 2002;33(9):2206-2210.

Filippi M, Rocca MA. MR imaging of multiple sclerosis. *Radiology.* 2011;259(3):659-681.

Finelli DA, Hurst GC, Gullapali RP, et al. Improved contrast of enhancing brain lesions on postgadolinium, T1-weighted spin-echo images with use of magnetization transfer. *Radiology.* 1994;190(2):553-559.

Firbank MJ, Blamire AM, Krishnan MS, et al. Diffusion tensor imaging in dementia with Lewy bodies and Alzheimer's disease. *Psychiatry Res.* 2007;155(2):135-145.

Forsting M, Palkowitsch P. Prevalence of acute adverse reactions to gadobutrol--a highly concentrated macrocyclic gadolinium chelate: review of 14,299 patients from observational trials. *Eur J Radiol.* 2010;74(3):e186-e192.

Freedman MS, Selchen D, Arnold DL, et al. Treatment optimization in MS: Canadian MS Working Group updated recommendations. *Can J Neurol Sci.* 2013;40(3):307-323.

Frenzel T, Lengsfeld P, Schirmer H, et al. Stability of gadolinium-based magnetic resonance imaging contrast agents in human serum at 37 degrees C. *Invest Radiol.* 2008;43(12):817-828.

Fries P, Runge VM, Bucker A, et al. Brain tumor enhancement in magnetic resonance imaging at 3 tesla: intraindividual comparison of two high relaxivity macromolecular contrast media with a standard extracellular gd-chelate in a rat brain tumor model. *Invest Radiol.* 2009;44(4):200-206.

Gadovist® [summary of product characteristics]. Berlin, Germany: Bayer Pharma AG; 2013.

Gao YZ, Zhang JJ, Liu H, et al. Regional cerebral blood flow and cerebrovascular reactivity in Alzheimer's disease and vascular dementia assessed by arterial spinlabeling magnetic resonance imaging. *Curr Neurovasc Res.* 2013;10(1):49-53.

Giesel FL, Mehndiratta A, Risse F, et al. Intraindividual comparison between gadopentetate dimeglumine and gadobutrol for magnetic resonance perfusion in normal brain and intracranial tumors at 3 Tesla. *Acta Radiol.* 2009;50(5):521-530.

Gillams AR, Fuleihan N, Grillone G, et al. Magnetization transfer contrast MR in lesions of the head and neck. *Am J Neuroradiol.* 1996;17(2):355-360.

Goyen M, Herborn CU, Vogt FM, et al. Using a 1 M Gd-chelate (gadobutrol) for total-body three-dimensional MR angiography: preliminary experience. *J Magn Reson Imaging.* 2003;17(5):565-571.

Gutierrez JE, Rosenberg M, Seeman J, et al. Safety and efficacy of gadobutrol for contrast-enhanced magnetic resonance imaging of the central nervous system: results from a multicenter, double-blind, randomized, comparator study. *MR Insights* 2014 (ahead of print).

Hadizadeh DR, Jost G, Pietsch H. Intra-individual quantitative and qualitative comparison of gadopentetate dimeglumine and gadobutrol in time-resolved contrast-enhanced 4D-MRA of minipigs. *Invest Radiol.* In press.

Hadizadeh DR, Kukuk GM, Steck DT, et al. Noninvasive evaluation of cerebral arteriovenous malformations by 4D-MRA for preoperative planning and postoperative follow-up in 56 patients: comparison with DSA and intraoperative findings. *Am J Neuroradiol.* 2012;33(6):1095-1101.

Hashemi H, Behzadi S, Ghanaati H, et al. Evaluation of plaque detection and optimum time of enhancement in acute attack multiple sclerosis after contrast injection. *Acta Radiol.* 2014 Mar;55(2):218-24.

Herborn CU, Lauenstein TC, Ruehm SG, et al. Intraindividual comparison of gadopentetate dimeglumine, gadobenate dimeglumine, and gadobutrol for pelvic 3D magnetic resonance angiography. *Invest Radiol.* 2003;38(1):27-33.

Huppertz A, Rohrer M. Gadobutrol, a highly concentrated MR-imaging contrast agent: its physicochemical characteristics and the basis for its use in contrast-enhanced MR angiography and perfusion imaging. *Eur Radiol.* 2004;14 Suppl 5:M12-M18.

Johnson KA, Fox NC, Sperling RA, et al. Brain imaging in Alzheimer disease. *Cold Spring Harb Perspect Med.* 2012;2(4):a006213.

Kastrup O, Wanke I, Maschke M. Neuroimaging of infections. *NeuroRx.* 2005;2(2):324-332.

Katakami N, Inaba Y, Sugata S, et al. Magnetic resonance evaluation of brain metastases from systemic malignances with two doses of gadobutrol 1.0 m compared with gadoteridol: a multicenter, phase ii/iii study in patients with known or suspected brain metastases. *Invest Radiol.* 2011;46(7):411-418.

Kidwell CS, Chalela JA, Saver JL, et al. Comparison of MRI and CT for detection of acute intracerebral hemorrhage. *JAMA.* 2004;292(15):1823-1830.

Kim ES, Chang JH, Choi HS, et al. Diagnostic yield of double-dose gadobutrol in the detection of brain metastasis: intraindividual comparison with double-dose gadopentetate dimeglumine. *Am J Neuroradiol.* 2010;31(6):1055-1058.

Koenig M, Schulte-Altedorneburg G, Heuser L. et al. Intraindividual, randomised comparison of the MRI contrast agents gadobutrol versus gadoteridol in patients with primary and secondary brain tumours, evaluated in blinded read. *Eur Radiol* 2013;23:3287–3295.

Kramer H, Runge VM, Morelli JN, et al. Magnetic resonance angiography of the carotid arteries: comparison of unenhanced and contrast enhanced techniques. *Eur Radiol.* 2011;21(8):1667-1676.

Kramer H, Runge VM, Naul LG, et al. Brain MRI with single-dose (0.1 mmol/kg) Gadobutrol at 1.5 T and 3 T: comparison with 0.15 mmol/kg Gadoterate meglumine. *Am J Roentgenol.* 2010;194(5):1337-1342.

Kramer JH, Arnoldi E, Francois CJ, et al. Dynamic and static magnetic resonance angiography of the supra-aortic vessels at 3.0 T: intraindividual comparison of gadobutrol, gadobenate dimeglumine, and gadoterate meglumine at equimolar dose. *Invest Radiol.* 2013;48(3):121-128.

Kukuk GM, Hadizadeh DR, Bostrom A, et al. Cerebral arteriovenous malformations at 3.0 T: intraindividual comparative study of 4D-MRA in combination with selective arterial spin labeling and digital subtraction angiography. *Invest Radiol.* 2010;45(3):126-132.

Lansberg MG, Lee J, Christensen S, et al. RAPID automated patient selection for reperfusion therapy: a pooled analysis of the Echoplanar Imaging Thrombolytic Evaluation Trial (EPITHET) and the Diffusion and Perfusion Imaging Evaluation for Understanding Stroke Evolution (DEFUSE) Study. *Stroke.* 2011;42(6):1608-1614.

Lansberg MG, Thijs VN, Hamilton S, et al. Evaluation of the clinical-diffusion and perfusion-diffusion mismatch models in DEFUSE. *Stroke.* 2007;38(6):1826-1830.

Law M, Meltzer DE, Cha S. Spectroscopic magnetic resonance imaging of a tumefactive demyelinating lesion. *Neuroradiology.* 2002;44(12):986-989.

Law M, Oh S, Babb JS, et al. Low-grade gliomas: dynamic susceptibility-weighted contrast-enhanced perfusion MR imaging--prediction of patient clinical response. *Radiology.* 2006;238(2):658-667.

Lawson MF, Velat GJ, Fargen KM, et al. Interventional neurovascular disease: avoidance and management of complications and review of the current literature. *J Neurosurg Sci.* 2011;55(3):233-242.

Lee YJ, Laub G, Jung SL, et al. Low-dose 3D time-resolved magnetic resonance angiography (MRA) of the supraaortic arteries: correlation with high spatial resolution 3D contrast-enhanced MRA. *J Magn Reson Imaging.* 2011;33(1):71-76.

Lövblad KO. Gadovist in multiple sclerosis. *Eur Neurol Rev.* 2008;3(1):59-60.

Lövblad KO, Anzalone N, Dorfler A, et al. MR imaging in multiple sclerosis: review and recommendations for current practice. *Am J Neuroradiol.* 2010;31(6):983-989.

Maravilla KR, Smith MR Pirovano G et al. Are there differences between macrocyclic Gadolinium contrast agents for brain tumor imaging ? results multicenter intraindividual crossover comparison of gadobutrol with gadoteridol (the TRUTH study). *Am Journal Neuroradiol* 2014 (ahead of print) Published October 9, 2014 as 10.3174/ajnr.A4154

Masdeu JC, Quinto C, Olivera C, et al. Open-ring imaging sign: highly specific for atypical brain demyelination. *Neurology.* 2000;54(7):1427-1433.

McDonald WI, Compston A, Edan G, et al. Recommended diagnostic criteria for multiple sclerosis: guidelines from the International Panel on the diagnosis of multiple sclerosis. *Ann Neurol.* 2001;50(1):121-127.

Menke J. Diagnostic accuracy of contrast-enhanced MR angiography in severe carotid stenosis: meta-analysis with metaregression of different techniques. *Eur Radiol.* 2009;19(9):2204-2216.

Mueller SG, Schuff N, Weiner MW. Evaluation of treatment effects in Alzheimer's and other neurodegenerative diseases by MRI and MRS. *NMR Biomed.* 2006;19(6):655-668.

Nagakane Y, Christensen S, Brekenfeld C, et al. EPITHET: Positive Result After Reanalysis Using Baseline Diffusion-Weighted Imaging/Perfusion-Weighted Imaging Co-Registration. *Stroke.* 2011;42(1):59-64.

Nicoletti G, Lodi R, Condino F, et al. Apparent diffusion coefficient measurements of the middle cerebellar peduncle differentiate the Parkinson variant of MSA from Parkinson's disease and progressive supranuclear palsy. *Brain.* 2006;129(Pt 10):2679-2687.

Nicoletti G, Tonon C, Lodi R, et al. Apparent diffusion coefficient of the superior cerebellar peduncle differentiates progressive supranuclear palsy from Parkinson's disease. *Mov Disord.* 2008;23(16):2370-2376.

Niethammer M, Feigin A, Eidelberg D. Functional neuroimaging in Parkinson's disease. *Cold Spring Harb Perspect Med.* 2012;2(5):a009274.

Olin JW, Kaufman JA, Bluemke DA, et al. Atherosclerotic Vascular Disease Conference: Writing Group IV: imaging. *Circulation.* 2004;109(21):2626-2633.

Paldino MJ, Barboriak DP. Fundamentals of quantitative dynamic contrast-enhanced MR imaging. *Magn Reson Imaging Clin N Am.* 2009;17(2):277-289.

Polman CH, Reingold SC, Banwell B, et al. Diagnostic criteria for multiple sclerosis: 2010 revisions to the McDonald criteria. *Ann Neurol.* 2011;69(2):292-302.

Port M, Corot C, Violas X, et al. How to compare the efficiency of albumin-bound and nonalbumin-bound contrast agents in vivo: the concept of dynamic relaxivity. *Invest Radiol.* 2005;40(9):565-573.

Rohrer M, Bauer H, Mintorovitch J, et al. Comparison of magnetic properties of MRI contrast media solutions at different magnetic field strengths. *Invest Radiol.* 2005;40(11):715-724.

Román G, Pascual B. Contribution of neuroimaging to the diagnosis of Alzheimer's disease and vascular dementia. *Arch Med Res.* 2012;43(8):671-676.

Rovira A, Auger C, Huerga E. MRI in clinically isolated syndromes and relapsing multiple sclerosis after single-dose and cumulative double-dose gadobutrol at 3.0 T: interim analysis. Abstract. RSNA 2011.

Rummeny EJ, Reimer P, Heindel W. *MR Imaging of the Body.* 1st ed. Stuttgart, Germany: Thieme Medical Publishers; 2009.

Runger VM. White matter disease and infection. In: Saunders WB, ed. *Clinical MRI.* Philadelphia: 2002.

Saur D, Kucinski T, Grzyska U, et al. Sensitivity and interrater agreement of CT and diffusion-weighted MR imaging in hyperacute stroke. *Am J Neuroradiol.* 2003;24(5):878-885.

Schellinger PD, Bryan RN, Caplan LR, et al. Evidence-based guideline: The role of diffusion and perfusion MRI for the diagnosis of acute ischemic stroke: report of the Therapeutics and Technology Assessment Subcommittee of the American Academy of Neurology. *Neurology.* 2010;75(2):177-185.

Schrag A, Good CD, Miszkiel K, et al. Differentiation of atypical parkinsonian syndromes with routine MRI. *Neurology.* 2000;54(3):697-702.

Seppi K, Schocke MF, Esterhammer R, et al. Diffusion-weighted imaging discriminates progressive supranuclear palsy from PD, but not from the parkinson variant of multiple system atrophy. *Neurology.* 2003;60(6):922-927.

Seute T, Leffers P, ten Velde GP, et al. Detection of brain metastases from small cell lung cancer: consequences of changing imaging techniques (CT versus MRI). *Cancer.* 2008;112(8):1827-1834.

Shiroishi S, Lacerda MS. Perfusion MRI of brain neoplasms. *Current Medical Imaging Reviews.* 2010;6(4):232-245.

Thomsen HS, Morcos SK, Almen T, et al. Nephrogenic systemic fibrosis and gadolinium-based contrast media: updated ESUR Contrast Medium Safety Committee guidelines. *Eur Radiol.* 2013;23(2):307-318.

Tombach B, Benner T, Reimer P, et al. Do highly concentrated gadolinium chelates improve MR brain perfusion imaging? Intraindividually controlled randomized crossover concentration comparison study of 0.5 versus 1.0 mol/L gadobutrol. *Radiology.* 2003;226(3):880-888.

Tombach B, Heindel W. Value of 1.0- M gadolinium chelates: review of preclinical and clinical data on gadobutrol. *Eur Radiol.* 2002;12(6):1550-1556.

Tsao MN, Rades D, Wirth A, et al. Radiotherapeutic and surgical management for newly diagnosed brain metastasis(es): An American Society for Radiation Oncology evidence-based guideline. *Pract Radiat Oncol.* 2012;2(3):210-225.

Tuite P, Mangia S, Michaeli S. Magnetic Resonance Imaging (MRI) in Parkinson's Disease. *J Alzheimers Dis.* 2013;S1:001.

Tunkel AR, Glaser CA, Bloch KC, et al. The management of encephalitis: clinical practice guidelines by the Infectious Diseases Society of America. *Clin Infect Dis.* 2008;47(3):303-327.

Uysal E, Erturk SM, Yildirim H, et al. Sensitivity of immediate and delayed gadolinium-enhanced MRI after injection of 0.5 M and 1.0 M gadolinium chelates for detecting multiple sclerosis lesions. *Am J Roentgenol.* 2007;188(3):697-702.

Vogler H, Platzek J, Schuhmann-Giampieri G, et al. Pre-clinical evaluation of gadobutrol: a new, neutral, extracellular contrast agent for magnetic resonance imaging. *Eur J Radiol.* 1995;21(1):1-10.

Voth M, Haneder S, Huck K, et al. Peripheral magnetic resonance angiography with continuous table movement in combination with high spatial and temporal resolution time-resolved MRA With a total single dose (0.1 mmol/kg) of gadobutrol at 3.0 T. *Invest Radiol.* 2009;44(9):627-633.

Voth M, Rosenberg M, Breuer J. Safety of gadobutrol, a new generation of contrast agents: experience from clinical trials and postmarketing surveillance. *Invest Radiol.* 2011;46(11):663-671.

Weishaupt D, Köchli VD, Marincek B. *How Does MRI Work? An Introduction to the Physics and Function of Magnetic Resonance Imaging.* 2nd ed. Berlin, Germany: Springer-Verlag; 2006.

Wikström J, Ronne-Engstrom E, Gal G, et al. Three-dimensional time-of-flight (3D TOF) magnetic resonance angiography (MRA) and contrast-enhanced MRA of intracranial aneurysms treated with platinum coils. *Acta Radiol.* 2008;49(2):190-196.

Wintermark M, Albers GW, Alexandrov AV, et al. Acute stroke imaging research roadmap. *Am J Neuroradiol.* 2008;29(5):e23-e30.

Yang CW, Carr JC, Futterer SF, et al. Contrast-enhanced MR angiography of the carotid and vertebrobasilar circulations. *Am J Neuroradiol.* 2005;26(8):2095-2101.

Appendix III: Gadovist® Dosing Recommendations*

Body weight (kg)	Standard Gadovist® dose	Higher Gadovist® doses	
	0.1 mmol/kg (=0.1 mL/kg)	0.2 mmol/kg (=0.2 mL/kg)	0.3 mmol/kg (=0.3 mL/kg)
30	3.0 mL	6.0 mL	9.0 mL
35	3.5 mL	7.0 mL	10.5 mL
40	4.0 mL	8.0 mL	12.0 mL
45	4.5 mL	9.0 mL	13.5 mL
50	5.0 mL	10.0 mL	15.0 mL
60	6.0 mL	12.0 mL	18.0 mL
70	7.0 mL	14.0 mL	21.0 mL
80	8.0 mL	16.0 mL	24.0 mL
90	9.0 mL	18.0 mL	27.0 mL
100	10.0 mL	20.0 mL	30.0 mL
110	11.0 mL	22.0 mL	33.0 mL
120	12.0 mL	24.0 mL	36.0 mL
130	13.0 mL	26.0 mL	39.0 mL
140	14.0 mL	28.0 mL	42.0 mL

Appendix 1 Volume of injection of Gadovist® based on body weight and dose: MRI applications in adults

* (Gadovist® 2013)

Body weight (kg)	Total volume (mL)	Body weight (kg)	Total volume (mL)
2.5	0.25	22.5	2.30
3.0	0.30	25.0	2.50
3.5	0.35	27.5	2.80
4.0	0.40	30.0	3.00
4.5	0.45	32.5	3.30
5.0	0.50	35.0	3.50
5.5	0.55	37.5	3.80
6.0	0.60	40.0	4.00
6.5	0.65	45.0	4.50
7.0	0.70	50.0	5.00
7.5	0.75	55.0	5.50
8.0	0.80	60.0	6.00
8.5	0.85	65.0	6.50
9.0	0.90	70.0	7.00
9.5	0.95	75.0	7.50
10.0	1.00	80.0	8.00
12.5	1.30	85.0	8.50
15.0	1.50	90.0	9.00
17.5	1.80	95.0	9.50
20.0	2.00	100.0	10.0

Appendix 2 Dosing of Gadovist® 1.0 injection by 0.1 mmol/kg body weight

Number of FOVs	<75 kg b.w.	≥75 kg b.w.
1 FOV (corresponding to 0.1–0.15 mmol/kg b.w.)	7.5 mL	10 mL
>1 FOV (corresponding to 0.2–0.3 mmol/kg b.w.)	15 mL	20 mL

Appendix 3 Recommended dosing of Gadovist®: cerebral MRA

Notes

Gadovist® 1.0 mmol / mL solution for injection. Composition: 1 mL solution for injection contains 604.72 mg gadobutrol (equiv. 1.0 mmol gadobutrol containing 157.25 mg gadolinium) as active ingredient. Excipient with known effect: 1 mL contains 0.00056 mmol (equivalent to 0.013 mg) of sodium. **Indications:** For diagnostic use only. Gadovist® is indicated in adults and children of all ages (including term neonates) for: 1.) Contrast enhancement in cranial and spinal magnetic resonance imaging (MRI); 2.) Contrast-enhanced MRI of liver or kidneys in patients with high suspicion or evidence of having focal lesions to classify these lesions as benign or malignant; 3.) Contrast enhancement in MR angiography; 4.) MR Imaging of pathologies of the whole body. Gadovist® facilitates visualisation of abnormal structures or lesions and helps in the differentiation between healthy and pathological tissue. Gadovist® should be used only when diagnostic information is essential and not available with unenhanced magnetic resonance imaging (MRI). Posology: Gadovist® should only be administered by healthcare professionals experienced in the field of clinical MRI practice. The lowest dose that provides sufficient enhancement for diagnostic purposes should be used. The dose should be calculated based on the patient's body weight, and should not exceed the recommended dose per kilogram of body weight detailed in this section. Gadovist® is for intravenous administration only. **Contraindications:** Hypersensitivity to the active substance or any of the excipients. **Special warnings and precautions for use:** While injecting Gadovist® into veins with a small lumen there is the possibility of adverse effects such as reddening and swelling. The usual safety requirements for MRI, especially the exclusion of ferromagnetic materials, also apply when using Gadovist®. Hypersensitivity reactions: As with other intravenous contrast agents, Gadovist® can be associated with anaphylactoid / hypersensitivity or other idiosyncratic reactions, characterized by cardiovascular, respiratory or cutaneous manifestations, and ranging to severe reactions including shock. In general, patients with cardiovascular disease are more susceptible to serious or even fatal outcomes of severe hypersensitivity reactions. The risk of hypersensitivity reactions may be higher in case of 1.) previous reaction to contrast media; 2.) history of bronchial asthma; 3.) history of allergic disorders. In patients with an allergic disposition the decision to use Gadovist® must be made after particularly careful evaluation of the risk-benefit ratio. Most of these reactions occur within half an hour of administration. Therefore, post-procedure observation of the patient is recommended. Medication for the treatment of hypersensitivity reactions as well as preparedness for institution of emergency measures are necessary. Delayed reactions (after hours up to several days) have been rarely observed. Impaired renal function: Prior to administration of Gadovist® it is recommended that all patients are screened for renal dysfunction by obtaining laboratory tests. There have been reports of nephrogenic systemic fibrosis (NSF) associated with use of some gadolinium-containing contrast agents in patients with acute or chronic severe renal impairment (GFR < 30 mL / min / 1.73 m2). Patients undergoing liver transplantation are at particular risk since the incidence of acute renal failure is high in this group. As there is a possibility that NSF may occur with Gadovist®, it should therefore only be used in patients with severe renal impairment and in patients in the perioperative liver transplantation period after careful risk / benefit assessment and if the diagnostic information is essential and not available with non-contrast enhanced MRI. Haemodialysis shortly after Gadovist® administration may be useful at removing Gadovist® from the body. There is no evidence to support the initiation of haemodialysis for prevention or treatment of NSF in patients not already undergoing haemodialysis. Neonates and infants: Due to immature renal function in neonates up to 4 weeks of age and infants up to 1 year of age, Gadovist® should only be used in these patients after careful consideration. Elderly: As the renal clearance of Gadovist® may be impaired in the elderly, it is particularly important to screen patients aged 65 years and older for renal dysfunction. Seizure disorders: Like with other gadolinium containing contrast agents special precaution is necessary in patients with a low threshold for seizures. Pregnancy and lactation: There are no data from the use of Gadovist® in pregnant women. Gadovist® should not be used during pregnancy unless the clinical condition of the woman requires use of Gadovist®. Continuing or discontinuing of breast feeding for a period of 24 hours after administration of Gadovist®, should be at the discretion of the doctor and lactating mother. **Undesirable effects:** The overall safety profile of Gadovist® is based on data from more than 6,300 patients in clinical trials and from post-marketing surveillance. The most frequently observed adverse drug reactions (≥ 0.5 %) in patients receiving Gadovist® are headache, nausea and dizziness. The most serious adverse drug reactions in patients receiving Gadovist® are cardiac arrest and severe anaphylactoid reactions (including respiratory arrest and anaphylactic shock). Delayed anaphylactoid reactions (hours later up to several days) have been rarely observed. Most of the undesirable effects were of mild to moderate intensity. Following adverse reactions have been observed: 1.) Common (≥ 1 / 100 to < 1 / 10) headache, nausea; 2.) Uncommon (≥ 1 / 1,000 to < 1 / 100) hypersensitivity/anaphylactoid reaction, dizziness, dysgeusia, paresthesia, dyspnea, vomiting, erythema, pruritus, rash, injection site reaction, feeling hot; 3.) Rare (≥ 1 / 10,000 to < 1 / 1,000) loss of consciousness, convulsion, parosmia, tachycardia, palpitations, dry mouth, malaise, feeling cold; 4.) Not known: cardiac arrest, NSF. Patients with an allergic disposition suffer more frequently than others from hypersensitivity reactions. Isolated cases of NSF have been reported with Gadovist®. Paediatric population: Frequency, type and severity of adverse reactions in children of all ages (including term neonates) are consistent with the adverse drug reaction profile known in adults. **Overdose:** The maximum daily single dose tested in humans is 1.5 mmol gadobutrol / kg body weight. No signs of intoxication from an overdose have so far been reported during clinical use. In case of inadvertent overdosage, cardiovascular monitoring (including ECG) and control of renal function is recommended as a measure of precaution. In case of overdose in patients with renal insufficiency, Gadovist® can be removed by haemodialysis. After 3 haemodialysis sessions approx. 98 % of the agent are removed from the body. However, there is no evidence that haemodialysis is suitable for prevention of NSF. Reporting of suspected adverse reactions: Healthcare professionals are asked to report any suspected adverse reactions via the national reporting system or to drugsafety.hk@bayer.com. **Date of revision of text:** Jan 2020. **Please note:** For current prescribing information refer to the package insert and / or contact your local Bayer HealthCare Organization: Bayer HealthCare Limited. 14/F Oxford House, Taikoo Place, 979 King's Road, Quarry Bay, Hong Kong.

Clear Direction. > From Diagnosis to Care.

14/F, Oxford House, Taikoo Place 979 King's Road, Quarry Bay, Hong Kong

Tel +852 8100 2755
Fax +852 3526 4762
E-mail bayerhkradiology@bayer.com
Webste: https://www.radiology.bayer.com. hk

PP-GAD-HK-0108-1